

JGR Biogeosciences



RESEARCH ARTICLE

10.1029/2025JG008872

Key Points:

- Bulk organic matter and leachates from terrestrial Pleistocene permafrost exhibit lower thermoreactivity than Holocene permafrost
- Organic matter source and transport distance on shelf collectively control organic matter thermoreactivity in shelf surface sediment
- The majority of reactive organic matter from terrestrial permafrost is degraded during transport on land or in nearshore coastal areas

Supporting Information:

Supporting Information may be found in the online version of this article.

Correspondence to:

G. Mollenhauer and T.-W. Lin, gesine.mollenhauer@awi.de; tsai-wen.lin@awi.de

Citation:

Lin, T.-W., Nehrke, G., Grotheer, H., Koch, B. P., Meyer, H., Ruben, M., et al. (2025). Holocene terrestrial permafrost contributes more highly reactive organic matter to the Laptev Sea shelf than Pleistocene permafrost. *Journal of Geophysical Research: Biogeosciences*, 130, e2025JG008872. https://doi.org/10.1029/2025JG008872

Received 21 FEB 2025 Accepted 24 SEP 2025

Author Contributions:

Conceptualization: Gesine Mollenhauer Data curation: Tsai-Wen Lin, Hendrik Grotheer, Jens Strauss Formal analysis: Tsai-Wen Lin, Gernot Nehrke, Hendrik Grotheer, Hanno Meyer, Manuel Ruben, Tommaso Tesi

Funding acquisition: Gesine Mollenhauer Investigation: Tsai-Wen Lin, Hendrik Grotheer, Ruediger Stein, Tommaso Tesi, Gesine Mollenhauer Methodology: Tsai-Wen Lin, Gernot Nehrke, Boris Peter Koch, Hanno Meyer, Tommaso Tesi

© 2025. The Author(s).

This is an open access article under the terms of the Creative Commons

Attribution License, which permits use, distribution and reproduction in any medium, provided the original work is properly cited.

Holocene Terrestrial Permafrost Contributes More Highly Reactive Organic Matter to the Laptev Sea Shelf Than Pleistocene Permafrost

Tsai-Wen Lin^{1,2} , Gernot Nehrke¹, Hendrik Grotheer^{1,2,3} , Boris Peter Koch^{1,4} , Hanno Meyer⁵ , Manuel Ruben¹ , Ruediger Stein^{1,2,3} , Jens Strauss⁵ , Tommaso Tesi⁶, and Gesine Mollenhauer^{1,2,3}

¹Alfred Wegener Institute, Helmholtz Centre for Polar and Marine Research, Bremerhaven, Germany, ²Department of Geosciences, University Bremen, Bremen, Germany, ³MARUM Centre for Marine Environmental Sciences, University Bremen, Bremen, Germany, ⁴University of Applied Sciences, Bremerhaven, Germany, ⁵Permafrost Research Section, Alfred Wegener Institute, Helmholtz Centre for Polar and Marine Research, Potsdam, Germany, ⁶Institute of Polar Sciences, National Research Council, Bologna, Italy

Abstract Warming can lead to mobilization of organic matter (OM) initially stored in circumarctic permafrost and subsequent greenhouse gas release to the atmosphere. Our understanding remains limited regarding how the extent of carbon release, that is, OM reactivity, varies across terrestrial permafrost types and how it changes during transport from land to marine shelves. In this study, we measured bulk organic (TOC, C/N), isotopic (δ^{13} C, Δ^{14} C), and thermogravimetric properties (TGA) as proxies of OM reactivity on bulk and water-soluble fractions (leachates) from terrestrial Holocene and Pleistocene permafrost, bulk surface sediments from the Laptev Sea, and sediment cores from the western Laptev Sea. Bulk OM from terrestrial Pleistocene permafrost exhibited lower reactivity compared to Holocene permafrost, as indicated by its lower thermoreactivity and more advanced degradation state, reflected in higher δ^{13} C values and lower C/N ratios. Marine surface sediments showed relatively old radiocarbon ages and reduced OM thermoreactivity in the eastern Laptev Sea shelf compared to the central and western Laptev Sea shelf. This likely resulted from a higher contribution of Pleistocene permafrost-derived OM. In the central and western Laptev Sea, a rapid decrease in OM thermoreactivity was observed near the coast, followed by a more gradual decline offshore. Downcore analyses revealed that the reduction in OM thermoreactivity primarily reflected degradation during cross-shelf transport rather than after burial. Our results advance the understanding of OM reactivity differences between Pleistocene and Holocene permafrost, as well as changes in terrestrial permafrost OM thermoreactivity during transport and post-burial.

Plain Language Summary Warming in the Arctic is releasing carbon from permafrost as microbes break down frozen soil, plants, and animal remains. To better understand this process, we studied how easily organic matter (OM) from both young and old terrestrial permafrost breaks down, as well as OM in surface and deeper sediments from the Laptev Sea shelf. We measured how easily the OM in these materials breaks down by examining the amount of the OM that decomposed at lower versus higher temperatures. On land, we found that old permafrost is more resistant to breakdown than young permafrost. In the eastern Laptev Sea shelf, surface sediments contained more OM from old, less degradable terrestrial permafrost. Moving westward, OM degradability decreases with increasing distance from the coast, suggesting rapid OM breakdown nearshore. Deeper sediment layers revealed that most OM degradation happened during transport from land to sea and across the shelf, with relatively little breakdown after burial. These findings improve our understanding of the differing vulnerabilities of young and old permafrost to degradation and emphasize the importance of transport processes in shaping OM reactivity distributions on Arctic Ocean marginal shelves.

1. Introduction

Vast quantities of aged carbon are sequestered in permafrost across the hinterlands of Siberia and Alaska (Strauss et al., 2017, 2021). These regions, which remained free from ice sheet cover during the last glacial maximum, allowed large-scale vegetation growth and soil accumulation (Dyke et al., 2003; Hughes et al., 2016). Thawing of this Pleistocene permafrost, together with Holocene permafrost, releases the carbon previously stored in permafrost back into active biogeochemical carbon cycles (Ruben et al., 2024; Schuur et al., 2015, 2022). This

LIN ET AL. 1 of 18



Journal of Geophysical Research: Biogeosciences

10.1029/2025JG008872

Resources: Manuel Ruben, Ruediger Stein, Jens Strauss, Gesine Mollenhauer Supervision: Gernot Nehrke, Gesine Mollenhauer Validation: Tsai-Wen Lin, Gernot Nehrke, Boris Peter Koch, Hanno Meyer, Ruediger Stein, Tommaso Tesi Visualization: Tsai-Wen Lin Writing - original draft: Tsai-Wen Lin Writing - review & editing: Tsai-Wen Lin, Gernot Nehrke, Hendrik Grotheer, Boris Peter Koch, Hanno Meyer, Manuel Ruben, Ruediger Stein, Jens Strauss, Tommaso Tesi, Gesine Mollenhauer

release may exacerbate the already rapid warming in the Arctic, where temperature increases are occurring at a rate about four times higher than the global average (Miller et al., 2010; Rantanen et al., 2022). Upon permafrost thawing, some carbon is emitted as greenhouse gases from degrading organic matter (OM) within short time spans after thawing, while the remainder is more recalcitrant and transported into terrestrial reservoirs such as rivers, where it may degrade further during transit or storage (Canuel & Hardison, 2016; LaRowe et al., 2020; Vonk & Gustafsson, 2013). Eventually, mobilized terrestrial permafrost is transported to marginal seas, including the Laptev Sea, and the majority of the deposited carbon on Arctic Ocean shelves originates from terrestrial OM (Karlsson et al., 2011; Martens et al., 2022, 2024; Sun et al., 2025).

A critical question is: How reactive is the OM, that is, how much of the carbon stored in different types of permafrost is likely to be released to the atmosphere as greenhouse gases upon permafrost thawing? Current evidence presents diverse perspectives. Some studies suggest high OM reactivity of Pleistocene permafrost compared to Holocene permafrost, based on higher amount of carbon release in the dissolved organic carbon (DOC) fraction (Drake et al., 2015; Mann et al., 2015, 2022; Spencer et al., 2015; Vonk et al., 2013) as well as lower initial degradation status inferred from biomarkers such as acetate (Stapel et al., 2018) and lignin phenols (Tesi et al., 2014; Winterfeld, Goñi, et al., 2015). Conversely, other studies report that Pleistocene permafrost is less bioavailable, based on incubation experiments (Gentsch et al., 2015; Kuhry et al., 2020; Martens et al., 2023; Melchert et al., 2022; Schädel et al., 2014), and more degraded than Holocene permafrost, as indicated by lower total organic carbon to total nitrogen (C/N) ratios, higher stable carbon isotope (δ^{13} C) values, and degraded biomarker indices (Schirrmeister et al., 2011; Strauss et al., 2015).

Another unresolved question is how mobilized terrestrial permafrost OM reactivity changes during cross-shelf transport. In marine surface sediments across the Laptev Sea shelf, OM degradation is evident from decreasing contents of terrigenous biomarkers (including long-chain n-alkanes, long-chain fatty acids, and lignin phenols), declining total organic carbon (TOC) contents, increasing δ^{13} C values, and enhanced terrestrial biomarker-based degradation indices (Alling et al., 2012; Bro der et al., 2018, 2016; Fahl et al., 2001; Fahl & Stein, 1997; Gershelis et al., 2020; Karlsson et al., 2011; Martens et al., 2024; Mueller-Lupp et al., 2000; Shulga et al., 2024; Sparkes et al., 2016; Stein & Fahl, 2000; Stein & Fahl, 2004; Tesi et al., 2016; Tesi et al., 2014; Vonk et al., 2012; Vonk et al., 2014). Although these indices provide insights into OM degradation during cross-shelf transport on the Laptev Sea shelf, the changes in bulk OM reactivity between terrestrial permafrost and marine surface sediments remain poorly understood. Moreover, only few studies have attempted to quantitatively assess the residual OM reactivity or the associated carbon loss in marine sediments during transport (Bröder et al., 2018; Martens et al., 2024; Tesi et al., 2014). To fill these knowledge gaps, we employed thermogravimetric analysis (TGA) to assess variations in the thermoreactivity of bulk OM from both terrestrial and marine materials. Thermoreactivity measured by TGA can reflect OM bioreactivity, as soil incubation experiments show that the bioactive OM loss during microbial degradation is reflected as decreasing thermoreactive (labile) OM content that decomposes at lower temperatures (Plante et al., 2009; Siewert et al., 2012; Tokarski et al., 2019). Similar trends have also been observed in pine forest litter and artificial compost, where more decomposed samples are associated with lower thermoreactive OM content (Dell'Abate et al., 2000; Royira et al., 2008). Owing to this relationship between thermoreactivity and bioreactivity, TGA provides a rapid quantitative assessment on bulk OM reactivity in supplement of incubation experiments. TGA requires small sample amount and minimal sample preparation (Plante et al., 2009; Siewert et al., 2012), and therefore has been applied to both soils (e.g., Lopez-Capel et al., 2005; Siewert et al., 2012; Tokarski et al., 2019) and marine sediments (e.g., Lopez-Capel et al., 2006; Smeaton & Austin, 2022; Smeaton & Austin, 2024).

This study investigates the OM reactivity in Holocene and Pleistocene terrestrial permafrost. We hypothesized that (a) Pleistocene terrestrial permafrost OM is less reactive than Holocene terrestrial permafrost OM (Figure 1a), and (b) thus, mobilized terrestrial Holocene permafrost contributes more reactive OM to Laptev Sea shelf sediments than Pleistocene terrestrial permafrost (Figure 1b). To test these hypotheses, we assessed OM thermoreactivity via TGA and compared it with TOC, C/N ratios, and δ^{13} C values of bulk OM from Pleistocene and Holocene terrestrial permafrost materials. In combination with radiocarbon analysis, we examined spatial differences in OM thermoreactivity related to variations in terrestrial input sources and cross-shelf changes in OM thermoreactivity in Laptev Sea surface sediments. Finally, we investigated key stages of OM thermoreactivity decrease along the permafrost mobilization pathways, from land to the Laptev Sea shelf, and subsequent deposition.

LIN ET AL. 2 of 18

21698961, 2025, 10, Downloaded from https://agupubs.onlinelibrary.wiley.com/doi/10.1029/2025JG008872 by Helmholtz-Zentrum Potsdam GFZ, Wiley Online Library on [28/11/2025]. See the "

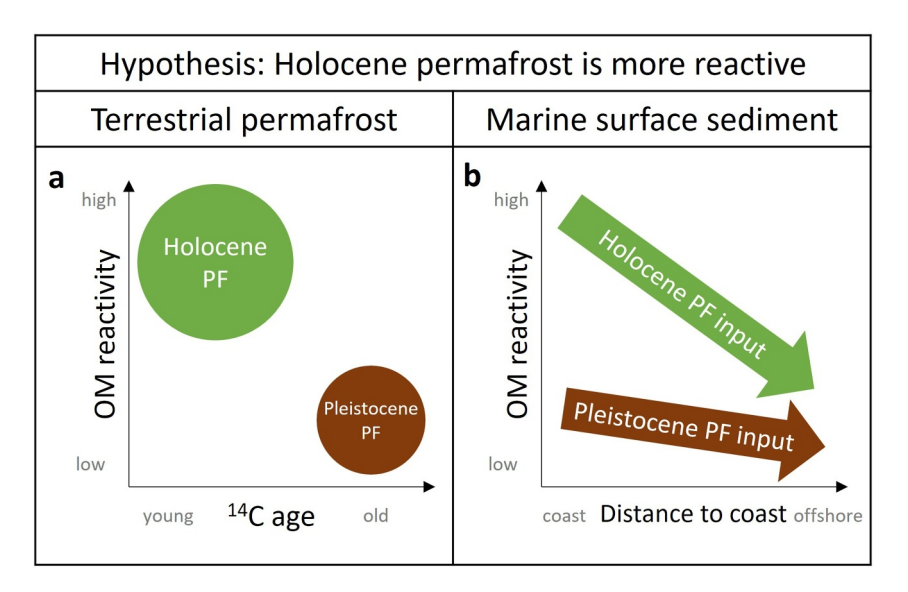


Figure 1. Conceptual diagrams illustrating changes in organic matter (OM) reactivity under the hypotheses that (a) Holocene permafrost contains more labile components and is overall more reactive than Pleistocene permafrost. (b) Holocene permafrost contributes more reactive OM to the marine surface sediments. The circle sizes in panel (a) are proportional to the size of the carbon stock in the Yedoma domain (in brown; carbon stock = 327-466 Pg; data from Strauss et al., 2017) and in soils from 0 to 3 m depth and deltaic alluvium (in green; carbon stock = 812.6 ± 136 Pg; data from Palmtag et al., 2022), respectively.

2. Study Area

The Laptev Sea coast and its hinterland are predominantly underlain by Pleistocene permafrost (Grigoriev et al., 2004; Strauss et al., 2021, 2022, 2025) (Figure 2). Overlying Pleistocene permafrost lies permafrost formed during the Holocene, on top of them is a seasonally thawed active layer (Harris et al., 1988). Permafrost is defined as soil that remains below 0°C for at least two consecutive years (Harris et al., 1988). The ice- and organic-rich permafrost formed during the late Pleistocene is specifically referred to as Yedoma (Strauss et al., 2015, 2021), and constitutes one of the major circumarctic carbon pools (Strauss et al., 2017, 2025). Collectively, Yedoma regions and drained thermokarst formed in Yedoma regions are referred to as the Yedoma domain (Strauss et al., 2017, 2025).

The Laptev Sea, a marginal sea of the Arctic Ocean (Figures 2a and 2b), receives substantial amounts of terrestrial OM from coastal erosion and Lena River discharge (Boucsein & Stein, 2000; Günther et al., 2013; Martens et al., 2024; McClelland et al., 2016). Terrestrial sources dominate organic carbon flux to the Laptev Sea shelf (Boucsein & Stein, 2000; Fahl et al., 2001; Fahl & Stein, 1997; Martens et al., 2022; Mueller-Lupp et al., 2000; Stein & Fahl, 2000), with approximately equal inputs from Pleistocene and Holocene permafrost (Martens et al., 2022). Riverine transport delivers over 2.5 times more organic carbon to the Laptev Sea than coastal erosion, though primarily in the form of DOC. Consequently, coastal erosion is the predominant source of particulate organic carbon, contributing about four times more compared to river discharge (Martens et al., 2024; Stein & Fahl, 2004). Annually, approximately 3.2 Tg (Tg) of particulate terrestrial organic carbon are transported to the Laptev Sea, with ~50% degraded during transport, ~13% buried in the shelf sediments, and the remainder exported to the continental slope or carried away by sea ice (Martens et al., 2024). The sediment depo-center of the Laptev Sea is located in areas with water depths of about 30 m (Bauch et al., 2001; Kuptsov & Lisitsin, 1996).

The Laptev Sea is ice-free for about 3 months each year, with sea ice covering it for most of the year (Fahl et al., 2001; Hörner et al., 2016). Ice algae assemblages are prevalent on the outer shelves of the central and western Laptev Sea (Fahl et al., 2001). Elevated marine primary productivity is observed from proxies in shelf surface sediments near the Lena Delta and polynyas (Fahl & Stein, 1997). Spatial differences in sediment sources are evident between the eastern and central-western Laptev Sea, as reflected by mineralogical assemblages of shelf surface sediments (Dethleff et al., 2000; Guay et al., 2001). The eastern Laptev Sea shelf receives more input from the Lena River, and most of the Lena River's discharge is further transported eastward and northward toward

LIN ET AL. 3 of 18

21698961, 2025, 10, Downloaded from https://agupubs.onlinelibrary.wikey.com/doi/10.1029/2025JG008872 by Helmholtz-Zentrum Potsdam GFZ, Wiley Online Library on [28/11/2025]. See the Terms

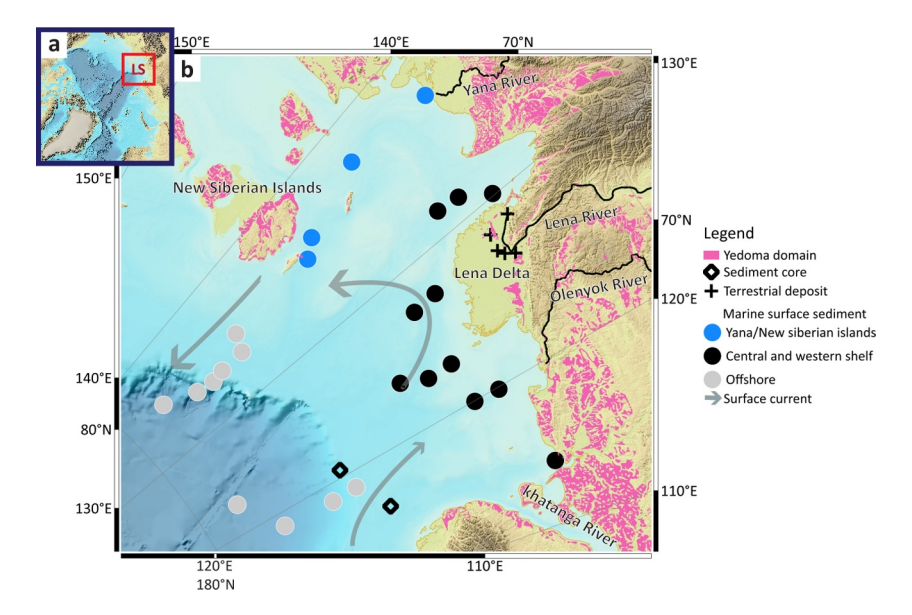


Figure 2. (a) Map of the Arctic Ocean in a polar projection, with the study area, the Laptev Sea (LS), highlighted in a red square. (b) Detailed map of the study area and sample locations. Samples include terrestrial permafrost from the Lena Delta (crosses), Laptev Sea surface sediments (dots), and two marine sediment cores (diamonds). Laptev Sea surface sediments are color-coded according to their geographical locations, with samples from the eastern Laptev Sea shelf (near Yana River mouth and new Siberian Islands) colored in light blue, samples from the central and western Laptev Sea shelves in black, and samples from the offshore Laptev Sea colored in light gray. The pink region shows the extent of the Yedoma domain (Strauss et al., 2016, 2021), gray arrows indicate the direction of marine surface current (Kleiber & Niessen, 2000), and black lines indicate major rivers (Lehner & Grill, 2013). Bathymetry data are sourced from the International Bathymetric Chart of the Arctic Ocean (IBCAO) (Jakobsson et al., 2012). The maps were created using QGIS3.22.9 (QGIS Geographic Information System. QGIS Association. https://www.qgis.org).

the Eastern Siberian Sea by local winds (Dmitrenko et al., 1999; Guay et al., 2001; Osadchiev et al., 2020). On the contrary, the western Laptev Sea receives freshwater from the Kara Sea, resulting in a higher marine influence in this region. These regional differences are reflected in zooplankton and phytoplankton communities (Fahl et al., 2001), δ^{13} C values of bulk OM (Fahl et al., 2001; Mueller-Lupp et al., 2000; Stein & Fahl, 2004), terrestrial (long-chain n-alkane) and marine (short-chain fatty acid) biomarker contents (Fahl et al., 2001; Fahl & Stein, 1997), diatom assemblages (Fahl et al., 2001), and surface water salinities (Bauch et al., 2004; Stein & Fahl, 2004).

During the last deglaciation, a large area of the Laptev Sea shelf was exposed above sea level (~115 m lower than present at 18 kyr BP), and the sea level rose to near-modern levels by around 4 kyr BP (Bauch et al., 2001; Klemann et al., 2015), consistent with global sea-level trends indicating a deceleration of sea-level rise after the mid-Holocene (Creel et al., 2024; Lambeck et al., 2014). Reconstruction of paleo sea levels in this region relies heavily on model simulations, due to the limited availability of material suitable for reconstructing relative sea-level changes, and the geodynamic complexity on an active continental margin (Baranskaya et al., 2018; Li et al., 2022). Nevertheless, the flat and shallow (<50 m) bathymetry of the shelf renders the coastline highly sensitive to sea-level fluctuations, as reflected in many sediment cores representing intervals from the last glacial maximum to the Holocene (Bauch et al., 2001; Hörner et al., 2016; Kuptsov & Lisitsin, 1996; Liu et al., 2022; Mueller-Lupp et al., 2000; Stein & Fahl, 2000, 2004).

3. Materials and Methods

3.1. Materials

The samples analyzed in this study include terrestrial permafrost from the Lena Delta, Laptev Sea surface sediments, and marine sediment cores from the western Laptev Sea (Figure 2b). The terrestrial permafrost samples were collected from the Lena Delta and consisted of three individual sample sets. (a) Four Holocene permafrost peat bluff profiles from the first terraces of the Lena Delta, collected in 2009 and 2010 using a hatchet and

LIN ET AL. 4 of 18

Table 1
Radiocarbon Dating and Geochemistry Results for Terrestrial Permafrost Leachates From the Lena Delta

Sample type	Sample ID	Bulk Δ^{14} C (‰)	Leachate Δ^{14} C (‰)	Bulk TOC (%)	DOC con. (mg g OC ⁻¹)	$\mathrm{OM_L}/\mathrm{OM}~(\%)$
Holocene	SAM18-1,725-727 cm	-547.4 ± 1.8	-492.5 ± 1.8	9.3	5.17	69.3
Holocene	SAM18-1,2254-2,256 cm	-665.0 ± 1.3	-658.2 ± 1.3	33.8	10.84	69.2
Pleistocene	CAC19-Y1-9	-990.1 ± 0.4	-834.6 ± 0.9	1.3	40.86	52.3 47.4 (duplicate)
Pleistocene	CAC19-Y1-14	-993.2 ± 0.3	-915.1 ± 0.6	5.2	26.26	48.9

Note. DOC con. indicates the content of water-soluble OC fraction in total organic carbon.

hammer. Detailed information on the peat samples is described in (Winterfeld, Goñi, et al., 2015). The samples were sieved to <2 mm, freeze-dried, and ground. (b) Two Yedoma ice complex profiles: core SOB18-07 was collected in 2018 using a SIPRE permafrost corer (Wetterich et al., 2019), and samples from profile CAC19-Y1 were obtained in 2019 using a gasoline-powered portable drilling apparatus (Fuchs et al., 2021). (c) Permafrost soils collected on Samoylov Island: samples were subsampled from sediment core SAM18-01, drilled with a Russian URB2-4T rig in 2018 (Jongejans et al., 2019). These subsampled aliquots of the Yedoma and Samoylov permafrost were stored at -20° C before being freeze-dried, ground, and analyzed.

Surface sediments (0–1 cm) from the Laptev Sea were collected during three expeditions: the *Polarstern* cruise ARK-IX/4 (PS27) in 1993 (Fütterer, 1994), the *Ivan Kireyev* cruise Transdrift-1 in 1993 (Kassens & Karpiy, 1994), and the *Polarstern* cruise ARK-XI/1 in 1995 (Rachor, 1997) (Figure 2b). The samples were obtained using various methods, including large box corers, multiple corers, and spade box corers. The sediments were dried right after subsampling and ground before analysis. The distance between sample locations and the nearest coastline were calculated using the software QGIS3.22.9 (QGIS Geographic Information System. QGIS Association. https://www.qgis.org), based on the bathymetry result from IBCAO (Jakobsson et al., 2012).

Two marine sediment cores were collected using Kasten corers during the Polarstern cruise ARK-XIV/1b (PS51 Transdrift-V) in 1998 (Figure 2b). Core PS51/154-11 (77.276°N, 120.610°E, water depth 270 m, abbreviated as PS51/154) was retrieved from the upper continental slope, while core PS51/159-10 (76.767°N, 116.032°E, water depth 60 m, abbreviated as PS51/159) was retrieved from the outer shelf (Fahrbach, 1998; Kassens, 2016). Sediment cores were stored at -20° C and moved to 4° C for subsampling. Sediment aliquots were sampled from the cores at 5-10 cm intervals using syringes, and were freeze-dried right after subsampling. Data from these two cores were combined due to their proximity and comparability (Hörner et al., 2016; Lin et al., 2025; Taldenkova et al., 2010). Samples from the slumping event layer between 530 and 540 cm in core PS51/154 were excluded due to distinct signals in grain size, TOC, and lignin phenol content, likely indicating sediment redeposition rather than paleoenvironmental conditions (Hörner et al., 2016; Lin et al., 2025; Taldenkova et al., 2010). Age models for both cores were adopted from Lin et al. (2025), and the combined record spanned from the early last deglaciation to the late Holocene. Distances from core locations to paleo coastlines at different sea levels during these periods were calculated based on the age model of the two cores established in Lin et al. (2025), modelled sea-level fluctuation in the Laptev Sea (Klemann et al., 2015), and current shelf bathymetry, assuming paleo coastlines followed the present-day bathymetric contours (Jakobsson et al., 2012). We are aware that this assumption of the paleo coastline does not account for coastal erosion processes that occurred during the last deglaciation. However, due to the limited constrains on geomorphological changes of the Arctic coastline during this period (Baranskaya et al., 2018; Li et al., 2022), it represents the best available approximation.

Water-soluble fractions (leachates) were obtained from four terrestrial permafrost, including two Holocene permafrost samples from core SAM18-1 and two Pleistocene Yedoma permafrost samples from profile CAC19-Y1 (Table 1). To measure DOC concentration, $\sim\!200$ mg of dried sediment was leached in 20 mL deionized water for 24 hr at 4°C, with intermittent shaking every 6–8 hr. The leachates were filtered through 0.7 μ m GF/F filters, acidified to pH 2 using 37% HCl, and analyzed by high-temperature catalytic combustion (Shimadzu, TOC-VCPN); for details, see Ksionzek et al. (2018). Based on measured DOC concentrations, the required sediment weight for leaching was calculated to extract 10 mg of DOC, resulting in sediment dry weights ranging from 3 to 19 g. The volume of deionized water used was calculated based on the TOC content of the samples, following a ratio of 1 g OC sediment to 200 mL deionized water, as described in Bristol et al. (2024). The leaching and

LIN ET AL. 5 of 18

filtering process was the same as described above. The filtered leachates were concentrated by rotary evaporation to reduce solution volume and freeze-dried to complete dryness for further radiocarbon dating and thermogravimetric analyses. A duplicate thermogravimetric analysis was performed on one Pleistocene terrestrial permafrost leachate sample.

3.2. Thermogravimetric Analysis (TGA)

TGA provides quantitative assessments of bulk OM thermoreactivity by measuring weight loss during controlled heating. OM decomposing at lower temperatures is considered more reactive and susceptible to microbial decomposition, while OM decomposing at higher temperatures is relatively inert (Barneto et al., 2009; Lopez-Capel et al., 2006; Manning et al., 2005; Plante et al., 2005; Schuur et al., 2015). TGA results provide an integrated measure of the overall thermoreactivity of organic matter. For instance, commonly seen highly thermoreactive compounds include fucoid sugars, glucose, and proteins, whereas lignin, humic acids, and coal exhibit lower thermoreactivity (Lopez-Capel et al., 2006; Manning et al., 2005; Smeaton & Austin, 2022). However, assigning specific TGA peaks to individual compounds remains challenging, as certain organic compounds can exhibit multiple peaks in TGA thermograms, and mixtures of different organic materials can shift the thermal behavior of individual components compared to analyzing them separately (Plante et al., 2009; Zimmermann et al., 1987).

For analysis, sediment samples (~20 mg) and dried terrestrial permafrost leachates (~10 mg) were analyzed in 70 μ L aluminum oxide crucibles using a Mettler Toledo TGA/DSC 1. Samples were heated from 25 to 1,000°C at a rate of 10°C min⁻¹ under a stable argon flow of 20 mL min⁻¹, following similar settings from previous studies (Smeaton & Austin, 2022, 2024). Prior to sample measurements, the weight change of an empty crucible was measured for calibration. OM was categorized into three fractions based on decomposition temperatures: labile (200–400°C), recalcitrant (400–550°C), and refractory (550–650°C) (Lopez-Capel et al., 2006) (Figure S1 in Supporting Information S1). Contents of labile OM fraction (OM_L) and the combined recalcitrant and refractory fractions (OM_R) were quantified in mg per g sediment, based on weight loss within these temperature ranges (Smeaton & Austin, 2022). The quantitation limit and precision of the TGA method is dependent on the balance type; in our case, the resolution of the balance is 0.1 μ g. Measurement uncertainties for OM_L and OM_R were both \pm 0.2 mg g sed⁻¹, calculated as the standard deviation (1 σ) of five replicate analyses of one marine core sediment sample. OM thermoreactivity was assessed as the fraction of labile OM relative to total OM (OM_L/OM), expressed as a percentage, modified from the index published by Smeaton and Austin (2022) (Equation 1). Higher OM_L/OM values indicate higher OM thermoreactivity. The measurement uncertainty for OM_L/OM was \pm 0.2%, based on the same replicate analyses written above.

$$\frac{OM_L}{OM} = \frac{OM_L}{OM_L + OM_R} \times 100 \,(\%) \tag{1}$$

3.3. Total Organic Carbon (TOC), Total Nitrogen (TN), and Stable Carbon (δ^{13} C) Analyses of Bulk OM in Sediments

Previously published TOC, C/N, and δ^{13} C data were incorporated for samples that had been analyzed, while new measurements were conducted for the remaining samples. For terrestrial permafrost from the Lena Delta, part of the TOC, C/N, and δ^{13} C values was from Winterfeld, Laepple, and Mollenhauer (2015). δ^{13} C values for eight Laptev Sea surface sediment samples were taken from Mueller-Lupp et al. (2000), and those for cores PS51/154 and PS51/159 were from (Lin et al., 2025). Additional δ^{13} C measurements for 14 Laptev Sea surface sediments were performed at the ISOLAB Facility in Potsdam, using a Thermo Fisher Scientific Delta-V-Advantage gas mass spectrometer equipped with a FLASH elemental analyzer EA 2000 and a CONFLO IV gas mixing system. Samples were acidified with 6 M HCl at 60°C for 3 hr, dried, homogenized, and weighed into tin capsules. Sample sizes varied according to TOC content, targeting 0.2 mg of organic carbon for each measurement. Control standards were run alongside the samples to correct δ^{13} C values. Three samples were measured in duplicate to assess reproducibility, with a standard deviation (1 σ) of <0.15%. Additional TOC, C/N, and δ^{13} C measurements of terrestrial permafrost, as well as δ^{13} C measurements for two additional Laptev Sea surface sediment samples (IK9340-GKG and PS2747-8a) were performed at CNR-ISP in Bologna. These samples were freeze-dried, homogenized, and weighed ~15 mg into silver boats. The samples were acidified with 1.5 M HCl and dried at 55°C. The analyses were conducted using a Thermo Fisher Scientific DeltaQ IRMS coupled with a FLASH 2000 CHNS

LIN ET AL. 6 of 18

Analyzer via a CONFLO IV gas mixing system. The measurement uncertainties were evaluated based on replicate measurements of in-house standard. For TOC it was <3% and for TN it was <4% of the respective measured values, based on the coefficient of variation. For δ^{13} C, the standard deviation (1 σ) was <0.1%. All δ^{13} C values are reported in per mil (‰) relative to the V-PDB standard.

3.4. Radiocarbon (Δ^{14} C) Analysis of Bulk OM in Sediments and Leachates

Radiocarbon data of bulk OM for Lena Delta permafrost have been partially published by Ruben et al. (2024) and Winterfeld, Laepple, and Mollenhauer (2015). Additional measurements for bulk OM Δ^{14} C values from Lena Delta permafrost, Laptev Sea surface sediments, and sediment cores PS51/154 and PS51/159 were performed at the AWI MICADAS laboratory in Bremerhaven, following protocols in Mollenhauer et al. (2021). Freeze-dried, ground sediments were weighed into silver boats, with sample sizes determined by TOC content to target 1 mg of organic carbon. Samples were acidified with three drops of 6 M HCl at 60°C three times with 1 hr reaction time between treatments, then oven-dried overnight at 60°C. Subsequently, samples together with silver boats were folded into tin boats and converted into graphite targets using an elemental analyzer (Elementar vario Isotope) coupled to an automated graphitization system (Ionplus AG, AGE-3) (Wacker et al., 2010). For terrestrial permafrost leachates, dried samples were weighed into tin boats and converted into graphite targets directly, following the same principle as described above. Radiocarbon isotopic ratios of the graphitized samples were measured using a MIni CArbon Dating System (MICADAS) at AWI, Bremerhaven (Mollenhauer et al., 2021). The radiocarbon results were reported as Δ^{14} C values, calculated from the measured fraction modern (F¹⁴C) results as Equation 2. The 1σ measurement uncertainty of Δ^{14} C values for all the measurements were <4.5%. The specific 1σ error ranges for $\Delta^{14}C$ values corresponding to individual datapoints are listed in Tables S2–S5 of Supporting Information S1.

$$\Delta^{14}C = (F^{14}C - 1) \times 1000\%$$
 (2)

For downcore records, the $\Delta^{14}C$ values at the time of sediment deposition ($\Delta^{14}C_{initial}$) were calculated using Equation 3 to account for radiocarbon decay from deposition to the present (Schefuß et al., 2016). This correction enables comparison with $\Delta^{14}C$ values from marine surface sediments. λ is the decay constant of ^{14}C (1/8,267 yr $^{-1}$). t is the time of deposition, according to the age-depth model (in yr BP) published by Lin et al. (2025).

$$\Delta^{14}C_{\text{initial}} = (F^{14}C e^{\lambda t} - 1) \times 1000\%$$
(3)

4. Results and Discussion

4.1. OM Reactivity of Pleistocene and Holocene Terrestrial Permafrost

Terrestrial permafrost samples from sites within the Yedoma and non-Yedoma domains exhibited no significant differences in TOC, OM_L/OM ratios, $\delta^{13}C$ values, or C/N ratios (Figure 3). However, notable differences in OM characteristics were observed between sample ages (Figure 3). In the following discussion, terrestrial permafrost is categorized into Pleistocene and Holocene groups based on radiocarbon age.

In bulk fractions, Pleistocene permafrost samples generally exhibited lower OM thermoreactivity and lower TOC content (average $OM_L/OM = 43.4 \pm 5.0\%$, average $TOC = 2.4 \pm 1.0\%$) compared to Holocene permafrost (average $OM_L/OM = 58.6 \pm 9.1\%$, average $TOC = 8.4 \pm 8.3\%$) (Figures 3a and 3b), suggesting that the OM in Pleistocene permafrost has undergone more extensive degradation, depleting the fraction of reactive OM. The positive correlation between TOC contents and OM_L/OM ratios indicated that the decrease in TOC was linked to reactive OM loss (Figure 3b). This is also seen in the higher OM_L content in Holocene permafrost compared to Pleistocene permafrost (Figure S2 in Supporting Information S1). The relationship between TOC and reactive OM loss has also been observed in soil samples from other mid- and high latitude regions (Kučerík et al., 2018). The advanced degradation of Pleistocene permafrost was further supported by its lower C/N ratios and narrower C/N ratio range among samples (average C/N = 11.6 \pm 2.4) compared to Holocene samples (average C/N = 27.5 \pm 8.8) (Figure 3c), aligning with findings from previous studies (Gentsch et al., 2015; Weiss et al., 2016). Lower C/N ratios in sediments may indicate a predominant organic matter source from bacteria and/

LIN ET AL. 7 of 18

3 yrary.wiley.com/doi/10.1029/2025JG008872 by Helmholtz-Zentrum Potsdam GFZ, Wiley Online Library on [28/11/2025]. See the Term

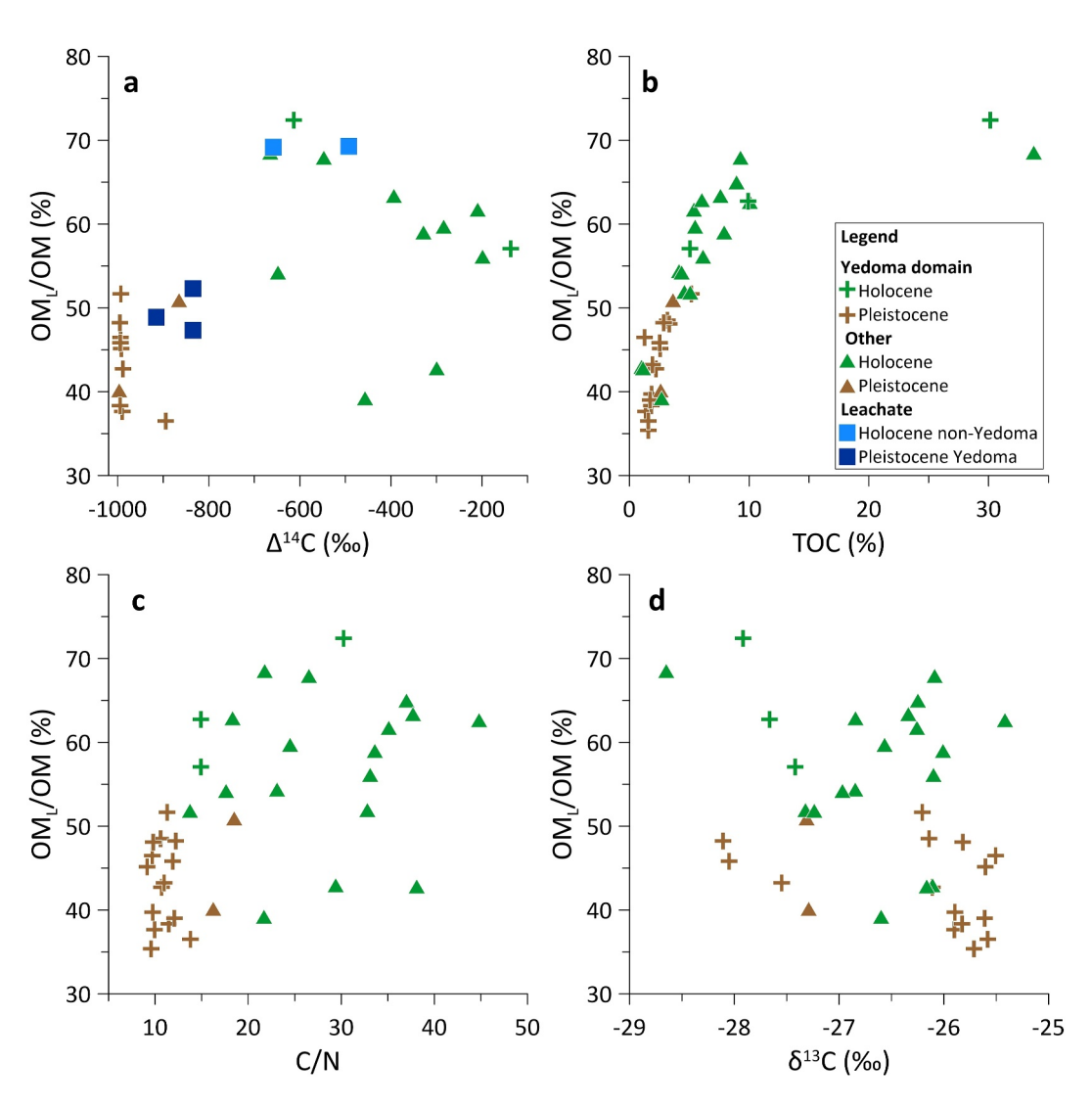


Figure 3. The percentage of labile organic matter (OM_L/OM) versus (a) bulk $\Delta^{14}C$ value, (b) total organic carbon (TOC, in % of dry weight), (c) C/N ratio, and (d) $\delta^{13}C$ value for terrestrial permafrost samples from the Lena Delta. The OM_L/OM result of Pleistocene Yedoma leachate in panel (a) includes duplicate measurements, for details see Table 1. Measurement uncertainties for individual data points are omitted from the figure due to their relative insignificance compared to the size of data points. For details on measurement uncertainties, see Chapter 3.

or algae, rather than from C_3 or C_4 plants (Lamb et al., 2006). Additionally, a decrease in C/N ratio can also result from microbial decomposition, which typically increases nitrogen content in soil and thus leads to lower C/N ratios (Bianchi & Canuel, 2011; Boström et al., 2007; Lamb et al., 2006). Furthermore, the low OM thermoreactivity in Pleistocene permafrost could be attributed to the high proportion of mineral-associated OM, which was either adsorbed onto clay-sized minerals or co-precipitated with hydrolysable iron minerals, protecting the OM from biodegradation (Gentsch et al., 2015; Martens et al., 2023; Salvadó et al., 2015). The δ^{13} C values of Pleistocene permafrost (average δ^{13} C = $-26.4 \pm 0.9\%$) (Figure 3d). Our observations differ from findings from the previous studies on the Lena Delta and Siberian hinterlands (Gentsch et al., 2015; Schirrmeister et al., 2011; Weiss et al., 2016), but aligns with data from the Lena Delta (Haugk et al., 2022) and the compiled terrestrial δ^{13} C records across Siberia (Martens et al., 2022). δ^{13} C values in soils and sediments reflect a complex interplay between organic matter sources and degradation processes (Bianchi & Canuel, 2011; Boström et al., 2007; Lamb et al., 2006), which may explain the lack of a consistent pattern in δ^{13} C across these studies. Our findings suggest that thermoreactivity in terrestrial permafrost is more closely associated with C/N ratios than with δ^{13} C values. The differences in OM_L/OM and C/N ratios between Holocene and Pleistocene permafrost might reflect inherent

LIN ET AL. 8 of 18

compositional characteristics, such as differences in terrestrial permafrost types or mineral association, or could also result from degradation on land after deposition. The latter is typically regarded to be minimal in permafrost as its frozen state slowed microbial decomposition (Schuur et al., 2008, 2015).

Leachates from terrestrial permafrost displayed consistent $\Delta^{14}C$ and OM_L/OM trends with the bulk fractions. Within our limited data set, Pleistocene permafrost leachates exhibited lower OM thermoreactivity than Holocene permafrost leachates (Figure 3a). Remarkably, Pleistocene Yedoma permafrost leachates showed higher $\Delta^{14}C$ values compared to the respective bulk materials and residual fractions after leaching (Figure 3a; Table 1; Figure S3a in Supporting Information S1). In contrast, Holocene permafrost displayed consistent $\Delta^{14}C$ values and OM_L/OM ratios between bulk samples, leachates, and leaching residuals (Table 1; Figure S3b in Supporting Information S1). The higher $\Delta^{14}C$ values in the Pleistocene permafrost leachates compared to its bulk materials suggested that in Pleistocene sediments, some DOC may have been leached downward from upper, younger horizons (Schuur et al., 2015). This was supported by higher DOC content in Pleistocene Yedoma compared to Holocene permafrost (Table 1).

Overall, the lower OM_L/OM and C/N ratios observed in Pleistocene permafrost compared to Holocene permafrost supported our hypothesis that Pleistocene terrestrial permafrost is generally less reactive than Holocene terrestrial permafrost (Figure 1a). These results were consistent with findings from incubation experiments of soils collected in multiple areas from Alaska and Eurasia (Gentsch et al., 2015; Kuhry et al., 2020; Melchert et al., 2022; Schädel et al., 2014). The higher OM reactivity of Holocene permafrost also explains observations of preferential microbial utilization of younger permafrost OM upon thawing (Melchert et al., 2022).

4.2. Spatial Variation of OM Reactivity in the Laptev Sea Surface

Significant regional differences were observed between surface sediments from the eastern Laptev Sea compared to the central and western Laptev Sea. Eastern Laptev Sea shelf sediments exhibited significantly lower bulk Δ^{14} C and OM₁/OM values than those from the central and western Laptev Sea shelves (Figures 4a and 4c; Figure 5). These low bulk Δ^{14} C values aligned with previous studies (Martens et al., 2021, 2022), suggesting a higher contribution of aged terrestrial OM, primarily from Yedoma domains including the North Siberian Islands and the Yana River catchment (Strauss et al., 2021) (Figures 4a and 4c). The overall higher sedimentation rate in the eastern Laptev Sea shelf relative to the central and western Laptev Sea shelves (Bauch et al., 2001; Fahl et al., 2001; Stein & Fahl, 2004) ruled out the possibility that older, less reactive sediment resulted from lower sedimentation rates and thus the 0-1 cm depth sample slice represented older sediment. A higher terrestrial OM input in the eastern Laptev Sea shelf was evident in previous studies, as indicated by higher terrestrial biomarker (long-chain n-alkanes, campesterol, β-sitosterol) contents, reduced marine biomarker (short-chain fatty acids) contents, and lower δ^{13} C values (Fahl et al., 2001; Fahl & Stein, 1997; Mueller-Lupp et al., 2000; Xiao et al., 2013). The low OM₁/OM ratios in the eastern Laptev Sea (Figures 5b and 5c), despite the limited datapoints, supported that Pleistocene terrestrial permafrost contributes less reactive OM to the Laptev Sea shelf than Holocene terrestrial permafrost (Figure 1b). This could be because of the inherently low OM reactivity of terrestrial Pleistocene permafrost (Chapter 4.1), or the OM in the eastern Laptev Sea shelf experienced further degradation in the water column compared to the central and western Laptev Sea, due to elevated microbial decomposition activities in this region (Fahl et al., 2001). On top of that increased input from marine primary production could stimulate the biodegradation activities of aged terrestrial permafrost in water column, known as the priming effect (Tesi et al., 2014).

Across regions receiving runoff from different rivers in the central and western Laptev Sea shelf, bulk $\Delta^{14}C$ and OM_L/OM ratios were relatively uniform, indicating similar OM sources across these regions compared to the eastern Laptev Sea (Figures 4a and 4c). Bulk $\delta^{13}C$ values increased from east to west across the Laptev Sea shelf, suggesting a westward gradient of increasing marine OM contributions (Fahl et al., 2001; Martens et al., 2022; Mueller-Lupp et al., 2000) (Figure 4b; Figure S4a in Supporting Information S1). If the terrestrial OM source supplying materials the central and western Laptev Sea was the same as the aged terrestrial OM input to the eastern Laptev Sea shelf, the increasing marine contribution would also result in a westward increase in $\Delta^{14}C$ values, as marine OM typically has higher $\Delta^{14}C$ values than Pleistocene permafrost (Martens et al., 2022). However, no correlation was observed between $\delta^{13}C$ and $\Delta^{14}C$ values in the shelf surface sediments (Figure S4b in Supporting Information S1). The terrestrial OM contribution to the Laptev Sea shelf, reflected in maceral compositions and rock-eval analysis, also showed no discernible east-west gradient (Boucsein & Stein, 2000;

LIN ET AL. 9 of 18

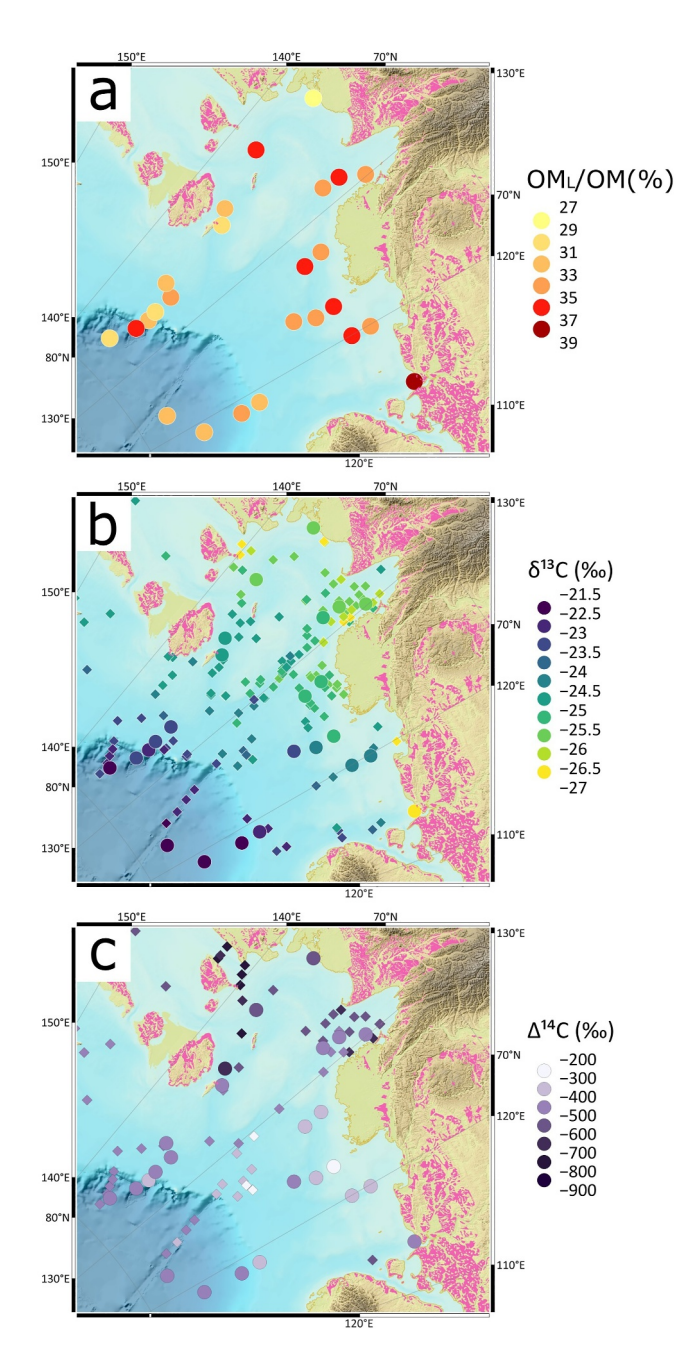


Figure 4. (a) The percentage of labile organic matter (OM_L/OM), (b) δ^{13} C values, and (c) radiocarbon Δ^{14} C values of the bulk fraction from Laptev Sea surface sediments, with dots representing data from this study and smaller diamonds representing data from previous studies (Fahl et al., 2001; Martens et al., 2021; Mueller-Lupp et al., 2000). The pink region shows the extent of the Yedoma domain (Strauss et al., 2016, 2021). Bathymetry data are sourced from the International Bathymetric Chart of the Arctic Ocean (IBCAO) (Jakobsson et al., 2012). The maps were created using QGIS3.22.9 (QGIS Geographic Information System. QGIS Association. https://www.qgis.org).

Fahl et al., 2001). These findings suggested that young radiocarbon ages (low Δ^{14} C values) in sediments from the central and western Laptev Sea resulted not only from differences in marine OM contributions, but also from inputs of younger terrestrial permafrost OM in contrast to the eastern Laptev Sea.

Coastal to offshore samples in the central and western Laptev Sea exhibited a decreasing trend in OM_I/OM ratios (Figure 5a), suggesting OM decomposition during cross-shelf transport (Tesi et al., 2016; Vonk et al., 2014). Our observations corroborate previous studies on offshore reduction in terrestrial OM content (Boucsein & Stein, 2000; Bröder et al., 2018, 2016; Fahl & Stein, 1997; Martens et al., 2024; Stein & Fahl, 2004; Tesi et al., 2016) and increased biomarker degradation (Broder et al., 2016; Fahl & Stein, 1997; Martens et al., 2024; Vonk et al., 2012). Increasing δ^{13} C values in offshore sediments in the Laptev Sea (Fahl et al., 2001; Mueller-Lupp et al., 2000) may reflect a shift toward marine OM input and/or enhanced OM degradation during transport (Lamb et al., 2006) (Figure 4b; Figure S4a in Supporting Information S1). If marine contributions dominated offshore OM, increases in OM_I/OM ratios and elevated bulk $\Delta^{14}C$ values would be expected, as marine algae typically produce highly reactive OM (LaRowe et al., 2020; Middelburg, 2019) and exhibit higher Δ^{14} C values than both Pleistocene and Holocene permafrost (Martens et al., 2022). However, the observed decrease in OM_I/OM ratios with increasing distance from the coast (Figure 5a) suggested that terrestrial OM degradation was the dominant process influencing the OM₁/OM ratios in Laptev Sea surface sediments, with limited contribution from reactive marine OM. This interpretation is supported by maceral composition from the Laptev Sea, which suggested that even in offshore locations, marine OM contributions to surface sediment did not exceed 20% (Boucsein & Stein, 2000). Additionally, the majority of marine OM is degraded in the water column before settling onto the sea bed (LaRowe et al., 2020; Shulga et al., 2024), with less than 0.5% of primary production in the Laptev Sea was buried in sediments (Stein & Fahl, 2004). The relatively stable Δ^{14} C values across the shelf in the central and western Laptev Sea might also indicate a limited role of marine OM input to the in-shelf transect (Figure 5c). Interestingly, Δ^{14} C values show little variation with coastal distance in this region, and a similar pattern was also observed in the Kara Sea (Martens et al., 2022). This lack of a clear trend may result from a balance between the aging of terrestrial OM and the input of young marine OM, or from other local environmental factors. However, further studies are needed to verify these inspections. Sedimentation rates can also influence marine surface sediment bulk Δ^{14} C values, as lower sedimentation rates may preserve older records within the 0-1 cm depth interval. Nonetheless, no systematic offshore decrease in sedimentation rates was observed in the central and western Laptev Sea (Bauch et al., 2001; Stein & Fahl, 2004), suggesting this effect is minimal. Overall, the observed cross-shelf decline in OM_I/OM ratios is best explained by cross-shelf terrestrial OM degradation, and less affected by other factors potentially affecting the bulk Δ^{14} C results. As water depth generally correlates with coastal distance, variations in OM_I/OM and δ^{13} C ratios in surface sediments from the Laptev Sea also showed depthrelated trends (Figure S5 in Supporting Information S1), albeit with weaker correlations (Table S1 in Supporting Information S1). Therefore, coastal distance was used as the primary parameter for comparison in this study.

Offshore samples from both the eastern and western Laptev Sea showed similar bulk Δ^{14} C values and OM_L/OM ratios (Figures 4a and 4c), with bulk Δ^{14} C values higher than those from the eastern Laptev Sea shelf (Figures 5a and 5c). This suggested that aged terrestrial OM from the eastern Laptev Sea shelf was not transported further

LIN ET AL. 10 of 18

21698961, 2025, 10, Downloaded from https://agupubs.onlinelibrary.wiley.com/doi/10.1029/2025JG008872 by Helmholtz-Zentrum

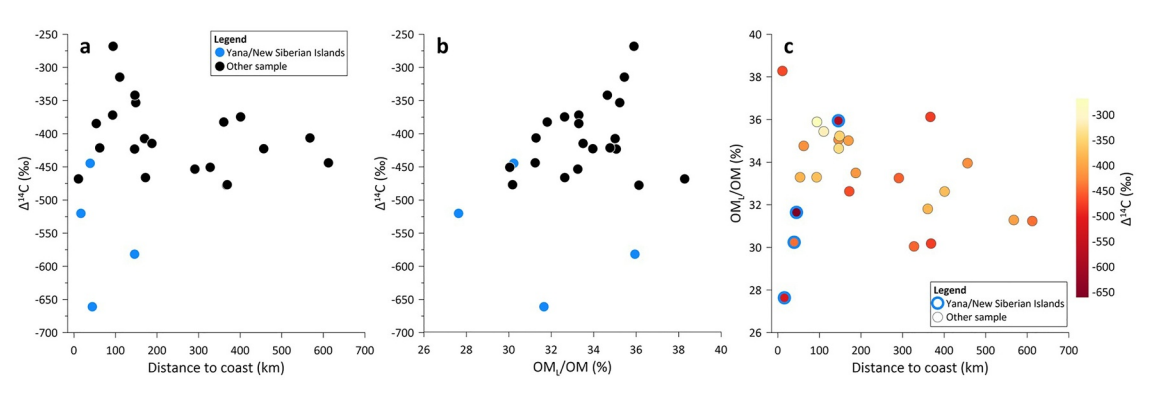


Figure 5. Cross plots of (a) bulk Δ^{14} C versus distance to the nearest coast, (b) bulk Δ^{14} C versus the percentage of labile organic matter (OM_L/OM), and (c) OM_L/OM versus distance to the nearest coast for Laptev Sea surface sediments. Sediments near the eastern Laptev Sea (Yana River mouth and the New Siberian Islands) are highlighted in blue. Measurement uncertainties for individual data points are omitted from the figure due to their relative insignificance compared to the size of data point markers. See Chapter 3 for further details on measurement uncertainties.

offshore, possibly due to eastward surface currents transporting material into the East Siberian Sea (Osadchiev et al., 2020). Retention of terrestrial OM on the eastern Laptev Sea shelf was supported by low bulk δ^{13} C values (Mueller-Lupp et al., 2000), high terrestrial biomarker contents (long-chain n-alkanes) (Fahl et al., 2001), and dominant terrestrial-sourced maceral compositions (Boucsein & Stein, 2000) in this region. Grain size difference might also play a role in cross-shelf OM thermoreactivity gradients. Low OM_L/OM ratios from the offshore Laptev Sea surface sediments were associated to a lower fractional abundance of sand in sediments (Fahl et al., 2001; Pantiukhin et al., 2019) (Figure S6 in Supporting Information S1). OM associated with fine particles could experience longer transport distances and repeated resuspension, resulting in increased degradation (Hare et al., 2014). In addition, plant debris retained on the inner shelf, which behaves hydraulically as sandy material, could further explain the decrease of OM thermoreactivity in offshore sediments (Tesi et al., 2016).

It is important to note that Laptev Sea surface sediments analyzed in this study were collected between 1993 and 1995 (Fütterer, 1994; Kassens & Karpiy, 1994; Rachor, 1997), when temperature and sea level in the Arctic were lower than today (Meredith et al., 2019). Recent warming can facilitate thermokarst development, exposing deeper permafrost (Schuur et al., 2008). Rising sea levels can accelerate coastal erosion along the Laptev Sea coast by increasing the fraction of inundated cliffs, making the immersed cliff more vulnerable to thermal denudation and abrasions (Nielsen et al., 2020, 2022; Rachold et al., 2000). Rapid increase in the coastal erosion rate along Arctic shorelines have been observed since the early to mid-2000s (Jones et al., 2020), and is projected to accelerate before the end of the 21st century (Nielsen et al., 2022). As a result, the Laptev Sea shelf today may receive a higher input of terrestrial OM input from deep permafrost than indicated by our findings.

4.3. OM Reactivity in Downcore Records

In cores PS51/154 and PS51/159, the OM_L/OM ratios exhibited a long-term decreasing trend from around 17.8 kyr BP at the bottom of the core to around 6 kyr BP, followed by an increase towards the most recent sediment most pronounced in core PS51/159 (Figure S8e in Supporting Information S1). Between 12 and 6.5 kyr BP, the Laptev Sea shelf was rapidly inundated, and the distances between paleo coastlines and sediment core sites increased (Jakobsson et al., 2012; Klemann et al., 2015) (Figures S7 and S8b in Supporting Information S1). As a result, OM_L/OM ratios in marine sediment core records might be influenced not only by OM decomposition after burial, but also by enhanced OM decomposition due to progressively increasing transport distances across the shelf. In cores PS51/154 and PS51/159 from the western Laptev Sea, higher OM_L/OM ratios were observed in samples closer to the coast (core bottom), and OM_L/OM ratios decreased with increasing distance from the coast (core tops) (Figure 7; Figures S8 and S9 in Supporting Information S1). The results suggested that low OM thermoreactivities in downcore records were driven primarily by degradation during elevated transport distance rather than longer post-depositional burial time. Sedimentary environments in the western Laptev Sea have undergone several variations since the last deglaciation. Ice-rafted debris (IRD) was identified in cores PS51/154 and PS51/159 during periods before 16 kyr BP and after 8 kyr BP (Taldenkova et al., 2010). Extensive sea-ice cover and reduced terrestrial OM input were found during periods before 16 kyr BP and Younger Dryas

LIN ET AL. 11 of 18

21698961, 2025, 10, Downloaded from https://agupubs.onlinelibrary.wiley.com/doi/10.1029/2025JG008872 by Helmholtz-Zentrum Potsdam GFZ, Wiley Online Library on [28/11/2025]. See the

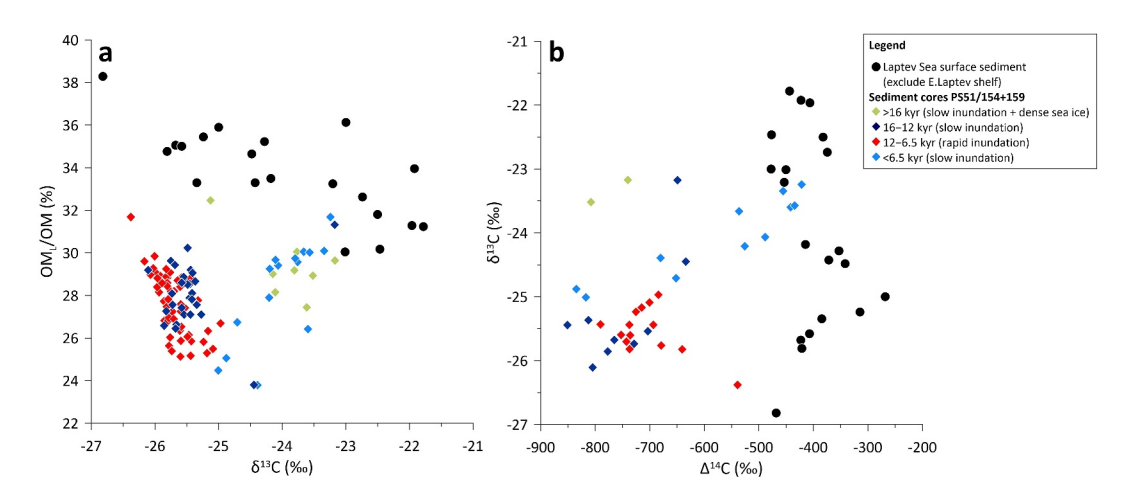


Figure 6. Cross plots of (a) the percentage of labile organic matter (OM $_{\rm L}$ /OM) versus stable carbon isotope (δ^{13} C) values and (b) δ^{13} C values versus radiocarbon isotope (Δ^{14} C) values in bulk sediments from the central and western Laptev Sea surface (dots) and cores PS51/154 and PS51/159 (diamonds). For the downcore records, the Δ^{14} C values are presented as the values at the time of sediment deposition (Δ^{14} C $_{\rm initial}$). Samples from cores PS51/154 and PS51/159 are color-coded based on periods with different shelf inundation rates (details in Figure S8 of Supporting Information S1). Measurement uncertainties for individual data points are omitted due to their relative insignificance compared to the size of the data point markers. See Chapter 3 for further details on measurement uncertainties.

(Hörner et al., 2016). In addition, three distinct events of enhanced terrestrial OM input were recorded in both sediment cores, coinciding with meltwater pulse events mwp-1a, mwp-1b, and the early Holocene (Hörner et al., 2016; Lin et al., 2025) (Figure S8c in Supporting Information S1). Interestingly, these pronounced environmental changes had minimal influence on downcore OM₁/OM variations in PS51/154 and PS51/159.

In downcore records, the relationships between OM_I/OM ratios, bulk δ^{13} C values, and bulk Δ^{14} C_{initial} values varied across different time periods (Figure 6). During the period of elevated shelf inundation between 12 and 6.5 kyr BP, OM_1/OM ratios decreased with increasing $\delta^{13}C$ values (red diamonds in Figure 6a; Figure S8 in Supporting Information S1). This trend resembled that observed in central and western Laptev Sea surface sediments, where offshore sediments exhibited lower OM_1/OM ratios and higher $\delta^{13}C$ values (Figure 5; black dots in Figure 6a; Figure S4 in Supporting Information S1). Unlike the correlation observed in the Laptev Sea surface, the δ^{13} C and Δ^{14} C_{initial} values exhibited little correlation in the downcore record during this period of extensive shelf inundation (Figure 6b; Figure S4b in Supporting Information S1). Given that several abrupt terrestrial permafrost mobilization events were observed during this period (Hörner et al., 2016; Lin et al., 2025) (Figure S8c in Supporting Information S1), the downcore $\Delta^{14}C_{initial}$ values may have been influenced not only by increased inundation but also by potential changes in the sources of terrestrial input. In contrast, during periods of slow inundation, an inverse correlation was observed between downcore OM_I/OM ratios, $\delta^{13}C$ values, and $\Delta^{14}C_{initial}$ values. Increased $\delta^{13}C$ values corresponded to elevated OM_{I}/OM ratios and higher $\Delta^{14}C_{initial}$ values (Figure 6; Figures S8d-S8f in Supporting Information S1), pointing to higher contributions from young and reactive marine OM. These downcore variations suggested that OM degradation during cross-shelf transport was the primary factor reducing OM reactivity. When transport distances remained relatively stable, enhanced marine primary productivity contributed younger and more reactive OM into shelf sediments, potentially caused by the warming during the last deglaciation and the Holocene (North Greenland Ice Core Project members, 2004) (Figure S8a in Supporting Information S1).

4.4. OM Degradation During Transport and Burial

In Laptev Sea surface sediments and marine sediment cores, we calculated the intercept of the linear OM_L/OM regression versus coastal distance, to estimate the theoretical OM_L/OM ratio at zero transport distance (Figure 7; Table 2). This approach eliminated the impact of degradation during cross-shelf transport. Marine sediment core data from the period of rapid shelf inundation rate were selected for the calculation, to eliminate the potential impact from temporal variations of marine primary production. Results calculated from full downcore records

LIN ET AL. 12 of 18

21698961, 2025, 10, Downloaded from https://agupubs.onlinelibrary.wiley.com/doi/10.1029/2025/G008872 by Helmholtz-Zentrum Potsdam GFZ, Wiley Online Library on [28/11/2025]. See the Terms and Condition

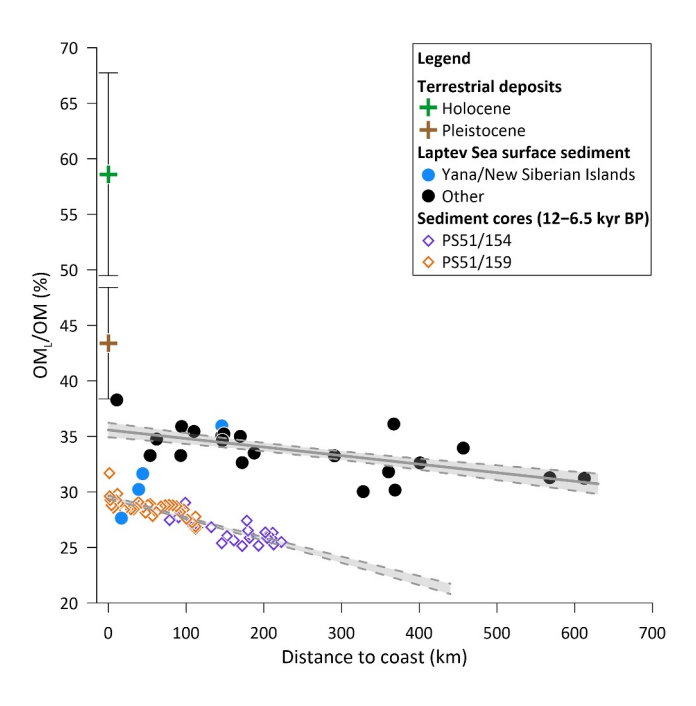


Figure 7. Percentage of labile organic matter (OM_L/OM) versus coastal distance. Crosses represent averages for Holocene (green) and Pleistocene (brown) terrestrial permafrost from the Lena Delta, with coastal distance set to zero. Circles represent Laptev Sea surface sediments, with samples near the Yana River mouth and the New Siberian Islands highlighted in blue. Diamonds represent results from marine sediment cores PS51/154 (purple) and PS51/159 (orange) from the period of rapid shelf inundation (12–6.5 kyr BP, detail in Figure S8 of Supporting Information S1, full data in Figure S9 of Supporting Information S1). Coastal distances for marine sediment cores were calculated based on paleo coastlines derived from paleo sea levels at the time of deposition (Klemann et al., 2015), assuming modern isobaths approximate paleo coastlines (Jakobsson et al., 2012). Gray lines represent linear regressions for Laptev Sea surface sediments (excluding samples from the Yana River and New Siberian Islands) and downcore records. Shaded gray bars show the 1σ confidence intervals for the regression lines. Measurement uncertainties for OM_L/OM ratios in surface sediments and downcore records are omitted due to their insignificance (uncertainties are smaller than the data point markers). For further information, see Chapter 3.

were listed in Table 2 for comparison, and the difference between the selected period and the full record was insignificant. A rapid decrease in OM_L/OM ratios was observed between terrestrial permafrost and marine surface sediments, with a more pronounced decrease for Holocene terrestrial permafrost (23%) compared to Pleistocene terrestrial permafrost (8%) (Table 2; Figure 7). The initial reactive OM loss likely reflected the rapid degradation of reactive OM pools, with degradation rates declining over time as these pools are depleted (Schuur et al., 2015). The variation in OM_L/OM ratios between coastal and offshore surface sediments in the Laptev Sea was relatively minor (Figure 7), suggesting that the majority of reactive OM decomposed near the coast shortly after entering the

Table 2Average Content of Labile Organic Matter (OM_L/OM) in Terrestrial Permafrost and Extrapolated OM_L/OM to a Coastal Distance of Zero (CD_0) in Marine Surface Sediment and Downcore Records

Samples	n	$\mathrm{OM_L/OM}$ (%)	$\mathrm{CD}_0\ \mathrm{OM_L/OM}\ (\%)$
Holocene terrestrial permafrost	21	58.6 ± 9.1	
Pleistocene terrestrial permafrost	17	43.4 ± 5.0	
Laptev Sea surface sediment	25		$34.1 \pm 0.8 \ (p > 0.05)$
Laptev Sea surface sediment (excluding New Siberian Islands)	21		$35.6 \pm 0.6 (p < 0.05)$
Downcore records	106		$29.0 \pm 0.2 \; (p < 0.05)$
Downcore records (12-6.5 kyr BP)	55		$29.5 \pm 0.2 \; (p < 0.05)$

Note. For terrestrial permafrost, the OM_L/OM ratio was calculated as the mean across all samples $\pm 1\sigma$ standard deviation. For marine surface sediments and downcore records, the CD_0 OM_L/OM ratio was derived from the intercept of the linear regression between OM_L/OM and coastal distance for each data point, representing the theoretical OM_L/OM value at zero coastal distance. Uncertainties are expressed as the standard error of the intercept.

LIN ET AL. 13 of 18

Acknowledgments

We thank the captains, the chief scientists,

the crews, and the scientific parties of the

ARK-XIV/1b (PS51 Transdrift-V) as well

RV Polarstern expeditions ARK-IX/4 (PS27), ARK-XI/1 (PS36), and

as the RV Ivan Kireyev Expedition:

CACOON project supported by the

Bundesministerium für Bildung und

Forschung (Grant 03F0806A) and the Natural Environment Research Council

(Grant NE/R012806/1) as part of the

Changing Arctic Ocean (CAO) program.

the German-Italian partnership project between the Alfred Wegener Institute and CNR-ISP on Chronologies for Polar

We thank Kirsten Fahl for providing coring information. This study was supported by

Paleoclimate Archives (PAIGE), funded by the Helmholtz Association (Grant PIE-

0018). We appreciate Arnaud Nicolas and Alessio Nogarotto's help in subsampling, and Jens Hefter, Laura Kattein, and Alessio

Nogarotto for their input and assistance in lab analysis. We thank Klaus-Uwe Richter

for the help in thermogravimetric analyses.

We appreciate Elizabeth Bonk and Torben Gentz for their assistance in sample pretreatment and radiocarbon analysis, and we thank Frederike Schmidt for the help in

DOC analysis and Mikaela Weiner for the δ^{13} C analyses. ChatGPT (version GPT-4)

was used in this manuscript to edit grammar

Access funding enabled and organized by

and improve sentence fluency. Open

Projekt DEAL.

Transdrift-1 for providing the studied material. Yedoma sampling was done in the sea shelf. This finding aligned with previous studies reporting rapid degradation of particulate OM during fluvial transport (Mann et al., 2015; Spencer et al., 2015), near-coastal shelf zones (Gershelis et al., 2020; Smeaton & Austin, 2022; Tanski et al., 2019; Tesi et al., 2014, 2016), and in the marine water column (Shulga et al., 2024). A decreasing trend in OM_I/OM ratios with increasing distance from the coast has also been observed in other midlatitude regions, including the Atlantic coast of Spain (Lopez-Capel et al., 2006) and the Scottish coast (Smeaton & Austin, 2022). The latter study additionally reported rapid degradation of thermoreactive OM in nearshore sediments. Compared to our findings, the magnitude of OM₁/OM decline from coastal to offshore samples appears greater in these mid-latitude regions. For example, OM₁/OM decreased from 44% to 19% off the Atlantic coast of Spain, and from $35 \pm 13\%$ inshore to $19 \pm 11\%$ offshore along the Scottish coast (Lopez-Capel et al., 2006; Smeaton & Austin, 2022). In contrast, the highest and the lowest OM_L/OM ratios in our coastal and offshore Laptev Sea samples were 38% and 30%, indicating a more moderate cross-shelf decline (Figure 7). This difference may be attributed to higher microbial activity in warmer mid-latitude environments, which enhance OM degradation (Gonzalez et al., 2015), or could be a result of regional variations in microbial community composition and environmental conditions.

An additional OM_I/OM decrease by 6% was observed between marine surface and downcore sediments (Table 2; Figure 7). The OM_I/OM decrease between the marine surface records and the downcore records might be caused by the intensified biodegradation in the oxic sediment layer in the surface sediments, as previous studies found rapid biodegradation happens within the topmost 1 cm of Laptev Sea sediment (Arndt et al., 2013; Kassens, 1997; Shulga et al., 2024). Alternatively, the higher OM_I/OM ratios in the surface sediments could result from higher marine OM contribution compared to the 12-6.5 kyr BP period recorded in the downcore records, due to the increasing marine primary production at the coring location in the late Holocene (Hörner et al., 2016).

5. Conclusions

Our findings in TGA confirmed that Pleistocene permafrost contains less reactive OM than Holocene permafrost, as reflected in both bulk and leachate fractions. Spatial difference of marine surface sediment OM thermoreactivity was found between the eastern from the central and western Laptev Sea shelves. The low OM thermoreactivity in the eastern Laptev Sea shelf likely resulted from higher contributions of aged, less reactive OM from Pleistocene permafrost and a higher bioactivity in this region, which might enhance OM biodegradation. In contrast, the central and western Laptev Sea shelves received more terrestrial input from Holocene permafrost, and offshore decreases in OM thermoreactivity in these regions were primarily attributed to terrestrial OM degradation during cross-shelf transport. Marine contributions appeared to have a limited impact on the OM thermoreactivity change of surface sediments in the Laptev Sea, compared to the degradation during transport. Changes in OM_I/OM ratios revealed a rapid decrease of thermoreactive OM in near-coastal regions, compared to the OM₁/OM decrease from the coast in Laptev Sea surface sediments. Our findings suggest that once permafrost thaws, the majority of its reactive carbon is likely to re-enter the active carbon cycle within a relatively short time, either on land or near shore. Subsequent degradation during cross-shelf transport and burial is less pronounced, though not negligible. To better understand the impacts of elevated inputs of aged terrestrial permafrost on OM degradation rates, further studies on the decomposition of aged permafrost in marine water columns are needed.

Conflict of Interest

The authors declare no conflicts of interest relevant to this study.

Data Availability Statement

All data are included in the Supporting Information S1 and additionally deposited in the publicly available PANGAEA Database (https://doi.org/10.1594/PANGAEA.984732).

References

Alling, V., Porcelli, D., Mörth, C. M., Anderson, L. G., Sanchez-Garcia, L., Gustafsson, Ö., et al. (2012). Degradation of terrestrial organic carbon, primary production and out-gassing of CO₂ in the Laptev and East Siberian Seas as inferred from δ^{13} C values of DIC. Geochimica et Cosmochimica Acta, 95, 143-159. https://doi.org/10.1016/j.gca.2012.07.028

Arndt, S., Jørgensen, B. B., LaRowe, D. E., Middelburg, J. J., Pancost, R. D., & Regnier, P. (2013). Quantifying the degradation of organic matter in marine sediments: A review and synthesis. Earth-Science Reviews, 123, 53-86. https://doi.org/10.1016/j.earscirev.2013.02.008

LIN ET AL. 14 of 18

- Baranskaya, A. V., Khan, N. S., Romanenko, F. A., Roy, K., Peltier, W. R., & Horton, B. P. (2018). A postglacial relative sea-level database for the Russian Arctic coast. *Quaternary Science Reviews*, 199, 188–205. https://doi.org/10.1016/j.quascirev.2018.07.033
- Barneto, A. G., Carmona, J. A., Alfonso, J. E. M., & Blanco, J. D. (2009). Kinetic models based in biomass components for the combustion and pyrolysis of sewage sludge and its compost. *Journal of Analytical and Applied Pyrolysis*, 86(1), 108–114. https://doi.org/10.1016/j.jaap.2009. 04.011
- Bauch, H. A., Erlenkeuser, H., Bauch, D., Mueller-Lupp, T., & Taldenkova, E. (2004). Stable oxygen and carbon isotopes in modern benthic foraminifera from the Laptev Sea shelf: Implications for reconstructing proglacial and profluvial environments in the Arctic. *Marine Micropaleontology*, 51(3–4), 285–300. https://doi.org/10.1016/j.marmicro.2004.01.002
- Bauch, H. A., Mueller-Lupp, T., Taldenkova, E., Spielhagen, R. F., Kassens, H., Grootes, P. M., et al. (2001). Chronology of the Holocene transgression at the North Siberian margin. *Global and Planetary Change*, 31(1–4), 125–139. https://doi.org/10.1016/S0921-8181(01)00116-3
- Bianchi, T. S., & Canuel, E. A. (2011). Chemical biomarkers in aquatic ecosystems. In *Chemical biomarkers in Aquatic ecosystems*. Princeton University Press, https://doi.org/10.5670/oceanog.2012.34
- Boström, B., Comstedt, D., & Ekblad, A. (2007). Isotope fractionation and ¹³C enrichment in soil profiles during the decomposition of soil organic matter. *Oecologia*, 153(1), 89–98. https://doi.org/10.1007/s00442-007-0700-8
- Boucsein, B., & Stein, R. (2000). Particulate organic matter in surface sediments of the Laptev Sea (Arctic Ocean): Application of maceral analysis as organic-carbon-source indicator. *Marine Geology*, 162(2–4), 573–586. https://doi.org/10.1016/S0025-3227(99)00066-3
- Bristol, E. M., Behnke, M. I., Spencer, R. G. M., McKenna, A., Jones, B. M., Bull, D. L., & McClelland, J. W. (2024). Eroding permafrost coastlines release biodegradable dissolved organic carbon to the Arctic Ocean. *Journal of Geophysical Research: Biogeosciences*, 129(7), e2024JG008233. https://doi.org/10.1029/2024jg008233
- Bröder, L., Tesi, T., Salvadó, J. A., Semiletov, I. P., Dudarev, O. V., & Gustafsson, O. (2016). Fate of terrigenous organic matter across the Laptev Sea from the mouth of the Lena River to the deep sea of the Arctic interior. *Biogeosciences*, 13(17), 5003–5019. https://doi.org/10.5194/bg-13-5003-2016
- Bröder, L., Tesi, T., Andersson, A., Semiletov, I., & Gustafsson, O. (2018). Bounding cross-shelf transport time and degradation in Siberian-Arctic land-ocean carbon transfer. *Nature Communications*, 9(1), 806. https://doi.org/10.1038/s41467-018-03192-1
- Canuel, E. A., & Hardison, A. K. (2016). Sources, ages, and alteration of organic matter in estuaries. Annual Review of Marine Science, 8(1), 409–434. https://doi.org/10.1146/annurey-marine-122414-034058
- Creel, R. C., Austermann, J., Kopp, R. E., Khan, N. S., Albrecht, T., & Kingslake, J. (2024). Global mean sea level likely higher than present during the Holocene. *Nature Communications*, 15(1), 10731. https://doi.org/10.1038/s41467-024-54535-0
- Dell'Abate, M., Benedetti, A., & Sequi, P. (2000). Thermal methods of organic matter maturation monitoring during a composting process. Journal of Thermal Analysis and Calorimetry, 61(2), 389–396. https://doi.org/10.1023/a:1010157115211
- Dethleff, D., Rachold, V., Tintelnot, M., & Antonow, M. (2000). Sea-ice transport of riverine particles from the Laptev Sea to Fram Strait based on clay mineral studies. *International Journal of Earth Sciences*, 89(3), 496–502. https://doi.org/10.1007/s005310000109
- Dmitrenko, I., Golovin, P., Gribanov, V., & Kassens, H. (1999). Oceanographic causes for transarctic ice transport of river discharge. In H. Kassens, H. A. Bauch, I. A. Dmitrenko, H. Eicken, H.-W. Hubberten, M. Melles, et al. (Eds.), *Land-Ocean systems in the Siberian arctic* (pp.
- 73–92). Springer. https://doi.org/10.1007/978-3-642-60134-7_9
 Drake, T. W., Wickland, K. P., Spencer, R. G., McKnight, D. M., & Striegl, R. G. (2015). Ancient low-molecular-weight organic acids in permafrost fuel rapid carbon dioxide production upon thaw. *Proceedings of the National Academy of Sciences of the United States of America* (Vol. 112(45), pp. 13946–13951). https://doi.org/10.1073/pnas.1511705112
- Dyke, A. S., Moore, A., & Robertson, L. (2003). Deglaciation of North America Open File 1574. https://doi.org/10.4095/214399
- Fahl, K., Cremer, H., Erlenkeuser, H., Hanssen, H., Hölemann, J., Kassens, H., et al. (2001). Sources and pathways of organic carbon in the modern Laptev Sea (Arctic Ocean): Implication from biological, geochemical and geological data. *Polarforschung*, 69, 193–205.
- Fahl, K., & Stein, R. (1997). Modern organic carbon deposition in the Laptev Sea and the adjacent continental slope: Surface water productivity vs. terrigenous input. *Organic Geochemistry*, 26(5–6), 379–390. https://doi.org/10.1016/S0146-6380(97)00007-7
- Fahrbach, E. (1998). FS "Polarstern" ARKTIS XIV/1a+b russisch-deutsche expeditionen (reports on polar research).
- Fuchs, M., Bolshiyanov, D., Grigoriev, M., Morgenstern, A., Pestryakova, L., Tsibizov, L., & Dill, A. (2021). Russian-German cooperation: Expeditions to Siberia in 2019 (1866–3192). (Berichte zur Polar-und Meeresforschung: Reports on Polar and Marine Research. https://doi.org/ 10.48433/BzPM 0749 2021
- Fütterer, D. K. (1994). The Expedition ARCTIC '93, leg ARK-IX/4 of RV "Polarstern" 1993. Reports on Polar Research. https://doi.org/10.2312/BzP 0149 1994
- Gentsch, N., Mikutta, R., Shibistova, O., Wild, B., Schnecker, J., Richter, A., et al. (2015). Properties and bioavailability of particulate and mineral-associated organic matter in Arctic permafrost soils, lower Kolyma Region, Russia. European Journal of Soil Science, 66(4), 722–734. https://doi.org/10.1111/ejss.12269
- Gershelis, E., Grinko, A., Oberemok, I., Klevantseva, E., Poltavskaya, N., Ruban, A., et al. (2020). Composition of sedimentary organic matter across the Laptev Sea shelf: Evidences from rock-eval parameters and molecular indicators. Water, 12(12), 3511. https://doi.org/10.3390/ w12123511
- Gonzalez, J., Portillo, M., & Piñeiro-Vidal, M. (2015). Latitude-dependent underestimation of microbial extracellular enzyme activity in soils. International journal of Environmental Science and Technology, 12(7), 2427–2434. https://doi.org/10.1007/s13762-014-0635-7
- Grigoriev, M. N., Rachold, V., Hubberten, H.-W., & Schirrmeister, L. (2004). Organic carbon input to the Arctic Seas through coastal erosion. In R. Stein & R. W. MacDonald (Eds.), *The organic carbon cycle in the Arctic Ocean* (pp. 41–45). Springer-Verlag. https://doi.org/10.1007/978-3-642-18912-8
- Guay, C. K., Falkner, K. K., Muench, R. D., Mensch, M., Frank, M., & Bayer, R. (2001). Wind-driven transport pathways for Eurasian Arctic river discharge. *Journal of Geophysical Research*, 106(C6), 11469–11480. https://doi.org/10.1029/2000JC000261
- Günther, F., Overduin, P. P., Sandakov, A. V., Grosse, G., & Grigoriev, M. N. (2013). Short- and long-term thermo-erosion of ice-rich permafrost coasts in the Laptev Sea region. *Biogeosciences*, 10(6), 4297–4318. https://doi.org/10.5194/bg-10-4297-2013
- Hare, A. A., Kuzyk, Z. Z. A., Macdonald, R. W., Sanei, H., Barber, D., Stern, G. A., & Wang, F. (2014). Characterization of sedimentary organic matter in recent marine sediments from Hudson Bay, Canada, by Rock-Eval pyrolysis. *Organic Geochemistry*, 68, 52–60. https://doi.org/10. 1016/j.orggeochem.2014.01.007
- Harris, S. A., French, H. M., Heginbottom, J. A., Johnston, G. H., Ladanyi, B., Sego, D. C., & van Everdingen, R. O. (1988). Glossary of permafrost and related ground-ice terms. National Research Council of Canada.
- Haugk, C., Jongejans, L. L., Mangelsdorf, K., Fuchs, M., Ogneva, O., Palmtag, J., et al. (2022). Organic matter characteristics of a rapidly eroding permafrost cliff in NE Siberia (Lena Delta, Laptev Sea region). Biogeosciences, 19(7), 2079–2094. https://doi.org/10.5194/bg-19-2079-2022

LIN ET AL. 15 of 18

- Hörner, T., Stein, R., Fahl, K., & Birgel, D. (2016). Post-glacial variability of sea ice cover, river run-off and biological production in the western Laptev Sea (Arctic Ocean): A high-resolution biomarker study. *Quaternary Science Reviews*, 143, 133–149. https://doi.org/10.1016/j. quascirev.2016.04.011
- Hughes, A. L., Gyllencreutz, R., Lohne, Ø. S., Mangerud, J., & Svendsen, J. I. (2016). The last Eurasian ice sheets: A chronological database and time-slice reconstruction, DATED-1. *Boreas*, 45(1), 1–45. https://doi.org/10.1111/bor.12142
- Jakobsson, M., Mayer, L., Coakley, B., Dowdeswell, J. A., Forbes, S., Fridman, B., et al. (2012). The International Bathymetric Chart of the Arctic Ocean (IBCAO) version 3.0. Geophysical Research Letters, 39(12). https://doi.org/10.1029/2012GL052219
- Jones, B. M., Irrgang, A. M., Farquharson, L. M., Lantuit, H., Whalen, D., Ogorodov, S., et al. (2020). Coastal permafrost erosion. Arctic report card, 15. https://doi.org/10.25923/e47w-dw52
- Jongejans, L. L., Assmann, V., Boike, J., Bolshiyanov, D., Bornemann, N., Grigoriev, B., et al. (2019). Research station Samoylov Island and Lena Delta, Samoylov deep drilling spring campaign 2018. In *Russian-German cooperation: Expeditions to Siberia in 2018* (Vol. 734, p. 257). Alfred Wegener Institute for Polar and Marine Research. https://doi.org/10.2312/BzPM 0734 2019
- Karlsson, E. S., Charkin, A., Dudarev, O., Semiletov, I., Vonk, J. E., Sánchez-García, L., et al. (2011). Carbon isotopes and lipid biomarker investigation of sources, transport and degradation of terrestrial organic matter in the Buor-Khaya Bay, SE Laptev Sea. *Biogeosciences*, 8(7), 1865–1879. https://doi.org/10.5194/bg-8-1865-2011
- Kassens, H. (1997). Laptev Sea System: Expeditions in 1995. Reports on Polar Research.
- Kassens, H. (2016). Station list and links to master tracks in different resolutions of POLARSTERN cruise ARK-XIV/1b, Tiksi-Tromsø, 1998-07-28–1998-08-28. PANGAEA. https://doi.org/10.1594/PANGAEA.858867
- Kassens, H., & Karpiy, V. Y. (1994). Russian-German cooperation: The transdrift I expedition to the Laptev Sea. Reports on Polar Research. https://doi.org/10.2312/BzP_0151_1994
- Kleiber, H. P., & Niessen, F. (2000). Variations of continental discharge pattern in space and time: Implications from the Laptev Sea continental margin, Arctic Siberia. *International Journal of Earth Sciences*, 89(3), 605–616. https://doi.org/10.1007/s005310000130
- Klemann, V., Heim, B., Bauch, H. A., Wetterich, S., & Opel, T. (2015). Sea-level evolution of the Laptev Sea and the East Siberian Sea since the last glacial maximum. *Arktos*, *I*(1), 1. https://doi.org/10.1007/s41063-015-0004-x
- Ksionzek, K. B., Zhang, J., Ludwichowski, K. U., Wilhelms-Dick, D., Trimborn, S., Jendrossek, T., et al. (2018). Stoichiometry, polarity, and organometallics in solid-phase extracted dissolved organic matter of the Elbe-Weser estuary. *PLoS One*, 13(9), e0203260. https://doi.org/10.1371/journal.pone.0203260
- Kučerík, J., Tokarski, D., Demyan, M. S., Merbach, I., & Siewert, C. (2018). Linking soil organic matter thermal stability with contents of clay, bound water, organic carbon and nitrogen. Geoderma, 316, 38–46. https://doi.org/10.1016/j.geoderma.2017.12.001
- Kuhry, P., Bárta, J., Blok, D., Elberling, B., Faucherre, S., Hugelius, G., et al. (2020). Lability classification of soil organic matter in the northern permafrost region. *Biogeosciences*, 17(2), 361–379. https://doi.org/10.5194/bg-17-361-2020
- Kuptsov, V., & Lisitsin, A. (1996). Radiocarbon of Quaternary along shore and bottom deposits of the Lena and the Laptev Sea sediments. Marine Chemistry, 53(3-4), 301-311. https://doi.org/10.1016/0304-4203(95)00096-8
- Lamb, A. L., Wilson, G. P., & Leng, M. J. (2006). A review of coastal palaeoclimate and relative sea-level reconstructions using δ¹³C and C/N ratios in organic material. Earth-Science Reviews, 75(1-4), 29–57. https://doi.org/10.1016/j.earscirev.2005.10.003
- Lambeck, K., Rouby, H., Purcell, A., Sun, Y., & Sambridge, M. (2014). Sea level and global ice volumes from the Last Glacial Maximum to the Holocene. Proceedings of the National Academy of Sciences of the United States of America (Vol. 111(43), pp. 15296–15303). https://doi.org/ 10.1073/pnas.1411762111
- LaRowe, D. E., Arndt, S., Bradley, J. A., Estes, E. R., Hoarfrost, A., Lang, S. Q., et al. (2020). The fate of organic carbon in marine sediments: New insights from recent data and analysis. *Earth-Science Reviews*, 204, 103146. https://doi.org/10.1016/j.earscirev.2020.103146
- Lehner, B., & Grill, G. (2013). Global river hydrography and network routing: Baseline data and new approaches to study the world's large river systems. *Hydrological Processes*, 27(15), 2171–2186. https://doi.org/10.1002/hyp.9740
- Li, T., Khan, N. S., Baranskaya, A. V., Shaw, T. A., Peltier, W. R., Stuhne, G. R., et al. (2022). Influence of 3D Earth structure on glacial isostatic adjustment in the Russian Arctic. *Journal of Geophysical Research: Solid Earth*, 127(3), e2021JB023631. https://doi.org/10.1029/2021jb023631
- Lin, T. W., Tesi, T., Hefter, J., Grotheer, H., Wollenburg, J., Adolphi, F., et al. (2025). Environmental controls of rapid terrestrial organic matter mobilization to the western Laptev Sea since the last deglaciation. Climate of the Past, 21(4), 753–772. https://doi.org/10.5194/cp-21-753-2025
- Liu, S., Wang, P., Huang, Q., Yu, J., Pozdniakov, S. P., & Kazak, E. S. (2022). Seasonal and spatial variations in riverine DOC exports in permafrost-dominated Arctic river basins. *Journal of Hydrology*, 612(Part C), 128060. https://doi.org/10.1016/j.jhydrol.2022.128060
- Lopez-Capel, E., de la Rosa Arranz, J. M., González-Vila, F. J., González-Perez, J. A., & Manning, D. A. C. (2006). Elucidation of different forms of organic carbon in marine sediments from the Atlantic coast of Spain using thermal analysis coupled to isotope ratio and quadrupole mass spectrometry. *Organic Geochemistry*, 37(12), 1983–1994. https://doi.org/10.1016/j.orggeochem.2006.07.025
- Lopez-Capel, E., Sohi, S. P., Gaunt, J. L., & Manning, D. A. C. (2005). Use of thermogravimetry-differential scanning calorimetry to characterize modelable soil organic matter fractions. Soil Science Society of America Journal, 69(1), 136–140. https://doi.org/10.2136/sssaj2005.0136a
- Mann, P. J., Eglinton, T. I., McIntyre, C. P., Zimov, N., Davydova, A., Vonk, J. E., et al. (2015). Utilization of ancient permafrost carbon in headwaters of Arctic fluvial networks. *Nature Communications*, 6(1), 7856. https://doi.org/10.1038/ncomms8856
- Mann, P. J., Strauss, J., Palmtag, J., Dowdy, K., Ogneva, O., Fuchs, M., et al. (2022). Degrading permafrost river catchments and their impact on Arctic Ocean nearshore processes. *Ambio*, 51(2), 439–455. https://doi.org/10.1007/s13280-021-01666-z
- Manning, D. A. C., Lopez-Capel, E., & Barker, S. (2005). Seeing soil carbon: Use of thermal analysis in the characterization of soil C reservoirs of differing stability. *Mineralogical Magazine*, 69(4), 425–435. https://doi.org/10.1180/0026461056940260
- Martens, J., Mueller, C. W., Joshi, P., Rosinger, C., Maisch, M., Kappler, A., et al. (2023). Stabilization of mineral-associated organic carbon in Pleistocene permafrost. *Nature Communications*, 14(1), 2120. https://doi.org/10.1038/s41467-023-37766-5
- Martens, J., Romankevich, E., Semiletov, I., Wild, B., van Dongen, B., Vonk, J., et al. (2021). CASCADE: The circum-arctic sediment carbon database. Earth System Science Data, 13(6), 2561–2572. https://doi.org/10.5194/essd-13-2561-2021
- Martens, J., Tesi, T., Rusakov, V., Semiletov, I., Dudarev, O., & Gustafsson, Ö. (2024). Off-shelf transport and biogeochemical cycling of terrestrial organic carbon along the East Siberian continental margin. Global Biogeochemical Cycles, 38(9), e2024GB008104. https://doi.org/ 10.1029/2024gb008104
- Martens, J., Wild, B., Semiletov, I., Dudarev, O. V., & Gustafsson, Ö. (2022). Circum-Arctic release of terrestrial carbon varies between regions and sources. Nature Communications, 13(1), 5858. https://doi.org/10.1038/s41467-022-33541-0
- McClelland, J. W., Holmes, R. M., Peterson, B. J., Raymond, P. A., Striegl, R. G., Zhulidov, A. V., et al. (2016). Particulate organic carbon and nitrogen export from major Arctic rivers. *Global Biogeochemical Cycles*, 30(5), 629–643. https://doi.org/10.1002/2015gb005351

LIN ET AL. 16 of 18

- Melchert, J. O., Wischhöfer, P., Knoblauch, C., Eckhardt, T., Liebner, S., & Rethemeyer, J. (2022). Sources of CO₂ produced in freshly thawed Pleistocene-age Yedoma permafrost. Frontiers in Earth Science, 9, 737237. https://doi.org/10.3389/feart.2021.737237
- Meredith, M., Sommerkorn, M., Cassotta, S., Derksen, C., Ekaykin, A., Hollowed, A., et al. (2019). Polar regions. In H.-O. Pörtner, D. C. Roberts, V. Masson-Delmotte, P. Zhai, M. Tignor, E. Poloczanska, et al. (Eds.), IPCC special report on the Ocean and Cryosphere in a changing climate (pp. 203–320). Cambridge University Press. https://doi.org/10.1017/9781009157964.005
- Middelburg, J. J. (2019). Marine carbon biogeochemistry: A primer for earth system scientists. Springer Nature. https://doi.org/10.1007/978-3-030-10822-9
- Miller, G. H., Alley, R. B., Brigham-Grette, J., Fitzpatrick, J. J., Polyak, L., Serreze, M. C., & White, J. W. C. (2010). Arctic amplification: Can the past constrain the future? *Quaternary Science Reviews*, 29(15–16), 1779–1790. https://doi.org/10.1016/j.quascirev.2010.02.008
- Mollenhauer, G., Grotheer, H., Gentz, T., Bonk, E., & Hefter, J. (2021). Standard operation procedures and performance of the MICADAS radiocarbon laboratory at Alfred Wegener Institute (AWI), Germany. *Nuclear Instruments and Methods in Physics Research Section B: Beam Interactions with Materials and Atoms*, 496, 45–51. https://doi.org/10.1016/j.nimb.2021.03.016
- Mueller-Lupp, T., Bauch, H. A., Erlenkeuser, H., Hefter, J., Kassens, H., & Thiede, J. (2000). Changes in the deposition of terrestrial organic matter on the Laptev Sea shelf during the Holocene: Evidence from stable carbon isotopes. *International Journal of Earth Sciences*, 89(3), 563– 568. https://doi.org/10.1007/s005310000128
- Nielsen, D. M., Dobrynin, M., Baehr, J., Razumov, S., & Grigoriev, M. (2020). Coastal erosion variability at the southern Laptev Sea linked to winter sea ice and the Arctic Oscillation. *Geophysical Research Letters*, 47(5), e2019GL086876. https://doi.org/10.1029/2019gl086876
- Nielsen, D. M., Pieper, P., Barkhordarian, A., Overduin, P., Ilyina, T., Brovkin, V., et al. (2022). Increase in Arctic coastal erosion and its sensitivity to warming in the twenty-first century. *Nature Climate Change*, 12(3), 263–270. https://doi.org/10.1038/s41558-022-01281-0
- North Greenland Ice Core Project members. (2004). High-resolution record of Northern Hemisphere climate extending into the last interglacial period. *Nature*, 431(7005), 147–151. https://doi.org/10.1038/nature02805
- Osadchiev, A. A., Pisareva, M. N., Spivak, E. A., Shchuka, S. A., & Semiletov, I. P. (2020). Freshwater transport between the Kara, Laptev, and East-Siberian seas. *Scientific Reports*, 10(1), 13041. https://doi.org/10.1038/s41598-020-70096-w
- Palmtag, J., Obu, J., Kuhry, P., Richter, A., Siewert, M. B., Weiss, N., et al. (2022). A high spatial resolution soil carbon and nitrogen dataset for the northern permafrost region based on circumpolar land cover upscaling. Earth System Science Data, 14(9), 4095–4110. https://doi.org/10. 5194/essd-14-4095-2022
- Pantiukhin, D., Popova, E., Piepenburg, D., & Kraan, C. (2019). Sand and silt distribution in the Eurasian Arctic, links to Geotiff. PANGAEA. https://doi.org/10.1594/PANGAEA.909391
- Plante, A. F., Fernández, J. M., & Leifeld, J. (2009). Application of thermal analysis techniques in soil science. *Geoderma*, 153(1–2), 1–10. https://doi.org/10.1016/j.geoderma.2009.08.016
- Plante, A. F., Pernes, M., & Chenu, C. (2005). Changes in clay-associated organic matter quality in a C depletion sequence as measured by differential thermal analyses. *Geoderma*, 129(3–4), 186–199. https://doi.org/10.1016/j.geoderma.2004.12.043
- Rachold, V., Grigoriev, M. N., Are, F. E., Solomon, S., Reimnitz, E., Kassens, H., & Antonow, M. (2000). Coastal erosion vs riverine sediment discharge in the Arctic Shelf seas. *International Journal of Earth Sciences*, 89(3), 450–460. https://doi.org/10.1007/s005310000113
- Rachor, E. (1997). Scientific criuse report of the Arctic expedition ARK-XI/1 of RV "Polarstern" in 1995 reports on Polar Research. https://doi.org/10.2312/BzP 0226 1997
- Rantanen, M., Karpechko, A. Y., Lipponen, A., Nordling, K., Hyvärinen, O., Ruosteenoja, K., et al. (2022). The Arctic has warmed nearly four times faster than the globe since 1979. Communications Earth and Environment, 3(1), 168. https://doi.org/10.1038/s43247-022-00498-3
- Rovira, P., Kurz-Besson, C., Coûteaux, M.-M., & Ramón Vallejo, V. (2008). Changes in litter properties during decomposition: A study by differential thermogravimetry and scanning calorimetry. Soil Biology and Biochemistry, 40(1), 172–185. https://doi.org/10.1016/j.soilbio. 2007.07.021
- Ruben, M., Marchant, H., Wietz, M., Gentz, T., Strauss, J., Koch, B. P., & Mollenhauer, G. (2024). Microbial communities degrade ancient permafrost-derived organic matter in Arctic seawater. *Journal of Geophysical Research: Biogeosciences*, 129(7), e2023JG007936. https://doi. org/10.1029/2023jg007936
- Salvadó, J. A., Tesi, T., Andersson, A., Ingri, J., Dudarev, O. V., Semiletov, I. P., & Gustafsson, Ö. (2015). Organic carbon remobilized from thawing permafrost is resequestered by reactive iron on the Eurasian Arctic Shelf. *Geophysical Research Letters*, 42(19), 8122–8130. https:// doi.org/10.1002/2015gl066058
- Schädel, C., Schuur, E. A., Bracho, R., Elberling, B., Knoblauch, C., Lee, H., et al. (2014). Circumpolar assessment of permafrost C quality and its vulnerability over time using long-term incubation data. *Global Change Biology*, 20(2), 641–652. https://doi.org/10.1111/gcb.12417
- Schefuß, E., Eglinton, T. I., Spencer-Jones, C. L., Rullkötter, J., De Pol-Holz, R., Talbot, H. M., et al. (2016). Hydrologic control of carbon cycling and aged carbon discharge in the Congo River basin. *Nature Geoscience*, 9(9), 687–690. https://doi.org/10.1038/ngeo2778
- Schirrmeister, L., Grosse, G., Wetterich, S., Overduin, P. P., Strauss, J., Schuur, E. A. G., & Hubberten, H.-W. (2011). Fossil organic matter characteristics in permafrost deposits of the northeast Siberian Arctic. *Journal of Geophysical Research*, 116, G00M02. https://doi.org/10. 1029/2011jg001647
- Schuur, E. A., Bockheim, J., Canadell, J. G., Euskirchen, E., Field, C. B., Goryachkin, S. V., et al. (2008). Vulnerability of permafrost carbon to climate change: Implications for the global carbon cycle. *BioScience*, 58(8), 701–714. https://doi.org/10.1641/B580807
- Schuur, E. A., McGuire, A. D., Schadel, C., Grosse, G., Harden, J. W., Hayes, D. J., et al. (2015). Climate change and the permafrost carbon feedback. *Nature*, 520(7546), 171–179. https://doi.org/10.1038/nature14338
- Schuur, E. A. G., Abbott, B. W., Commane, R., Ernakovich, J., Euskirchen, E., Hugelius, G., et al. (2022). Permafrost and climate change: Carbon cycle feedbacks from the warming arctic. *Annual Review of Environment and Resources*, 47(1), 343–371. https://doi.org/10.1146/annurevenviron-012220-011847
- Shulga, N. A., Romankevich, E. A., Vylegzhanina, N. V., Streltsova, E. A., Fedulov, V. Y., & Polyakova, A. V. (2024). Geochemical markers of organic matter transformation in the Eastern Laptev Sea. *Oceanology*, 64(2), 237–249. https://doi.org/10.1134/s0001437024020115
- Siewert, C., Demyan, M. S., & Kučerík, J. (2012). Interrelations between soil respiration and its thermal stability. *Journal of Thermal Analysis and Calorimetry*, 110(1), 413–419. https://doi.org/10.1007/s10973-011-2099-z
- Smeaton, C., & Austin, W. (2024). Potential effects of bottom trawling on organic carbon stocks in Denmark's marine sediments. D. Naturfredningsforening. https://doi.org/10.5281/zenodo.10075722
- Smeaton, C., & Austin, W. E. N. (2022). Quality not quantity: Prioritizing the management of sedimentary organic matter across continental shelf seas. Geophysical Research Letters, 49(5), e2021GL097481. https://doi.org/10.1029/2021gl097481
- Sparkes, R. B., Doğrul Selver, A., Gustafsson, Ö., Semiletov, I. P., Haghipour, N., Wacker, L., et al. (2016). Macromolecular composition of terrestrial and marine organic matter in sediments across the East Siberian Arctic Shelf. *The Cryosphere*, 10(5), 2485–2500. https://doi.org/10.5194/tc-10-2485-2016

LIN ET AL. 17 of 18

- Spencer, R. G. M., Mann, P. J., Dittmar, T., Eglinton, T. I., McIntyre, C., Holmes, R. M., et al. (2015). Detecting the signature of permafrost thaw in Arctic rivers. *Geophysical Research Letters*, 42(8), 2830–2835. https://doi.org/10.1002/2015gl063498
- Stapel, J. G., Schwamborn, G., Schirrmeister, L., Horsfield, B., & Mangelsdorf, K. (2018). Substrate potential of last interglacial to Holocene permafrost organic matter for future microbial greenhouse gas production. *Biogeosciences*, 15(7), 1969–1985. https://doi.org/10.5194/bg-15-1969-2018
- Stein, R., & Fahl, K. (2000). Holocene accumulation of organic carbon at the Laptev Sea continental margin (Arctic Ocean): Sources, pathways, and sinks. Geo-Marine Letters, 20(1), 27–36. https://doi.org/10.1007/s003670000028
- Stein, R., & Fahl, K. (2004). The Laptev Sea: Distribution, sources, variability and burial of organic carbon. In R. Stein & R. W. MacDonald (Eds.), The organic carbon cycle in the Arctic Ocean (pp. 213–237). Springer-Verlag, https://doi.org/10.1007/978-3-642-18912-8
- Strauss, J., Fuchs, M., Hugelius, G., Miesner, F., Nitze, I., Opfergelt, S., et al. (2025). Organic matter storage and vulnerability in the permafrost domain. In Encyclopedia of Quaternary science (pp. 399–410). https://doi.org/10.1016/b978-0-323-99931-1.00164-1
- Strauss, J., Laboor, S., Fedorov, A. N., Fortier, D., Froese, D. G., Fuchs, M., et al. (2016). Database of Ice-Rich Yedoma Permafrost (IRYP). https://doi.org/10.1594/PANGAEA.861733
- Strauss, J., Laboor, S., Schirrmeister, L., Fedorov, A. N., Fortier, D., Froese, D., et al. (2021). Circum-Arctic map of the Yedoma permafrost domain. Frontiers in Earth Science, 9, 758360. https://doi.org/10.3389/feart.2021.758360
- Strauss, J., Laboor, S., Schirrmeister, L., Fedorov, A. N., Fortier, D., Froese, D. G., et al. (2022). Database of ice-rich Yedoma Permafrost Version 2 (IRYP v2). PANGAEA. https://doi.org/10.1594/PANGAEA.940078
- Strauss, J., Schirrmeister, L., Grosse, G., Fortier, D., Hugelius, G., Knoblauch, C., et al. (2017). Deep Yedoma permafrost: A synthesis of depositional characteristics and carbon vulnerability. Earth-Science Reviews, 172, 75–86. https://doi.org/10.1016/j.earscirev.2017.07.007
- Strauss, J., Schirrmeister, L., Mangelsdorf, K., Eichhorn, L., Wetterich, S., & Herzschuh, U. (2015). Organic-matter quality of deep permafrost carbon: A study from Arctic Siberia. *Biogeosciences*, 12(7), 2227–2245. https://doi.org/10.5194/bg-12-2227-2015
- Sun, Y., Du, J., Hu, L., Zhang, Y., Ye, J., Zhu, C., et al. (2025). Spatial heterogeneity of terrestrial organic carbon burial and degradation in the East Siberian Arctic Shelf area. *Geochemistry, Geophysics, Geosystems*, 26(3), e2024GC011775. https://doi.org/10.1029/2024gc011775
- Taldenkova, E., Bauch, H. A., Gottschalk, J., Nikolaev, S., Rostovtseva, Y., Pogodina, I., et al. (2010). History of ice-rafting and water mass evolution at the northern Siberian continental margin (Laptev Sea) during late Glacial and Holocene times. *Quaternary Science Reviews*, 29(27–28), 3919–3935, https://doi.org/10.1016/j.guascirev.2010.09.013
- Tanski, G., Wagner, D., Knoblauch, C., Fritz, M., Sachs, T., & Lantuit, H. (2019). Rapid CO₂ release from eroding permafrost in seawater. Geophysical Research Letters, 46(20), 11244–11252. https://doi.org/10.1029/2019gl084303
- Tesi, T., Semiletov, I., Dudarev, O., Andersson, A., & Gustafsson, Ö. (2016). Matrix association effects on hydrodynamic sorting and degradation of terrestrial organic matter during cross-shelf transport in the Laptev and East Siberian shelf seas. *Journal of Geophysical Research: Biogeosciences*, 121(3), 731–752. https://doi.org/10.1002/2015jg003067
- Tesi, T., Semiletov, I., Hugelius, G., Dudarev, O., Kuhry, P., & Gustafsson, Ö. (2014). Composition and fate of terrigenous organic matter along the Arctic land-ocean continuum in East Siberia: Insights from biomarkers and carbon isotopes. *Geochimica et Cosmochimica Acta*, 133, 235–256. https://doi.org/10.1016/j.gca.2014.02.045
- Tokarski, D., Šimečková, J., Kučerík, J., Kalbitz, K., Demyan, M. S., Merbach, I., et al. (2019). Detectability of degradable organic matter in agricultural soils by thermogravimetry. *Journal of Plant Nutrition and Soil Science*, 182(5), 729–740. https://doi.org/10.1002/jpln.201800516
- Vonk, J. E., & Gustafsson, Ö. (2013). Permafrost-carbon complexities. Nature Geoscience, 6(9), 675–676. https://doi.org/10.1038/ngeo1937
 Vonk, J. E., Mann, P. J., Davydov, S., Davydova, A., Spencer, R. G. M., Schade, J., et al. (2013). High biolability of ancient permafrost carbon upon thaw. Geophysical Research Letters, 40(11), 2689–2693. https://doi.org/10.1002/grl.50348
- Vonk, J. E., Sanchez-Garcia, L., van Dongen, B. E., Alling, V., Kosmach, D., Charkin, A., et al. (2012). Activation of old carbon by erosion of coastal and subsea permafrost in Arctic Siberia. *Nature*, 489(7414), 137–140. https://doi.org/10.1038/nature11392
- Vonk, J. E., Semiletov, I. P., Dudarev, O. V., Eglinton, T. I., Andersson, A., Shakhova, N., et al. (2014). Preferential burial of permafrost-derived organic carbon in Siberian-Arctic shelf waters. *Journal of Geophysical Research: Oceans*, 119(12), 8410–8421. https://doi.org/10.1002/
- Wacker, L., Němec, M., & Bourquin, J. (2010). A revolutionary graphitisation system: Fully automated, compact and simple. *Nuclear Instruments and Methods in Physics Research Section B: Beam Interactions with Materials and Atoms*, 268(7–8), 931–934. https://doi.org/10.1016/j.nimb.
- Weiss, N., Blok, D., Elberling, B., Hugelius, G., Jørgensen, C. J., Siewert, M. B., & Kuhry, P. (2016). Thermokarst dynamics and soil organic matter characteristics controlling initial carbon release from permafrost soils in the Siberian Yedoma region. *Sedimentary Geology*, 340, 38–48. https://doi.org/10.1016/j.sedgeo.2015.12.004
- Wetterich, S., Kizyakov, A., Fritz, M., Aksenov, A., Schirrmeister, L., & Opel, T. (2019). Research station Samoylov Island and Lena Delta, permafrost research on Sobo-Sise Island (Lena Delta). *Russian-German cooperation: expeditions to Siberia in 2018* (Vol. 734, p. 257). Alfred Wegener Institute for Polar and Marine Research. https://doi.org/10.2312/BzPM_0734_2019
- Winterfeld, M., Goñi, M. A., Just, J., Hefter, J., & Mollenhauer, G. (2015). Characterization of particulate organic matter in the Lena River Delta and adjacent nearshore zone, NE Siberia—Part 2: Lignin-derived phenol compositions. *Biogeosciences*, 12(7), 2261–2283. https://doi.org/10.5194/bg-12-2261-2015
- Winterfeld, M., Laepple, T., & Mollenhauer, G. (2015b). Characterization of particulate organic matter in the Lena River Delta and adjacent nearshore zone, NE Siberia—Part I: Radiocarbon inventories. *Biogeosciences*, 12(12), 3769–3788. https://doi.org/10.5194/bg-12-3769-2015
- Xiao, X., Fahl, K., & Stein, R. (2013). Biomarker distributions in surface sediments from the Kara and Laptev seas (Arctic Ocean): Indicators for organic-carbon sources and sea-ice coverage. *Quaternary Science Reviews*, 79, 40–52. https://doi.org/10.1016/j.quascirev.2012.11.028
- Zimmermann, G., Lean, D., & Charlton, M. (1987). Differential thermal and thermogravimetric analysis of sediment-forming materials from Lake Ontario. Canadian Journal of Fisheries and Aquatic Sciences, 44(12), 2216–2224. https://doi.org/10.1139/f87-272

LIN ET AL. 18 of 18